ISTANBUL TECHNICAL UNIVERSITY ★ GRADUATE SCHOOL OF SCIENCE ENGINEERING AND TECHNOLOGY

CONTRIBUTION OF MXENE COATINGS TO THE PERFORMANCE OF NICKEL BASED ELECTROACTIVE MATERIALS

M.Sc. THESIS

BERKE KARAMAN

Metallurgical and Materials Engineering Department

Materials Engineering

JULY 2020

ISTANBUL TECHNICAL UNIVERSITY ★ GRADUATE SCHOOL OF SCIENCE ENGINEERING AND TECHNOLOGY

CONTRIBUTION OF MXENE COATINGS TO THE PERFORMANCE OF NICKEL BASED ELECTROACTIVE MATERIALS

M.Sc. THESIS

BERKE KARAMAN
506408181

Metallurgical and Materials Engineering Department

Materials Engineering Programme

Thesis Advisor: Prof. Dr. Mustafa Ürgen

2020 JULY

ISTANBUL TEKNİK ÜNİVERSİTESİ ★ FEN BİLİMLERİ ENSTİTÜSÜ

MXENE KAPLAMALARIN NİKEL BAZLI ELEKTROAKTİF MALZEMELEREİN PERFORMANSINA ETKİSİ

YÜKSEK LİSANS TEZİ

Berke KARAMAN
506181408

Metalurji ve Malzeme Mühendisliği Ana Bilim Dalı

Malzeme Mühendisliği Programı

Tez Danışmanı: Prof. Dr. Mustafa ÜRGEN

TEMMUZ 2020

Berke Karaman, a M.Sc. student of İTU Graduate School of Science Engineering and Technology student 506181408, successfully defended the thesis/dissertation entitled "CONTRIBUTION OF MXENE COATINGS TO THE PEFORMANCE OF NICKEL BASED ELECTROACTIVE MATERIALS", which he prepared after fulfilling the requirements specified in the associated legislations, before the jury whose signatures are below.

Thesis Advisor :	**Prof. Dr. Mustafa ÜRGEN** İstanbul Technical University	.....
Jury Members :	**Prof. Dr. Kürşat Kazmanlı** Istanbul Technical University	.....
	Dr. Fatma Bayata İstanbul Bilgi University	.....

Date of Submission : 15 June 2020
Date of Defense : 7 July 2020

To my mom, father and köpük,

FOREWORD

This thesis is the final work of my Master's study at the Istanbul Technical University, Materials Engineering programme from September 2018 to June 2020. This study provides information about the contribution of mxene coatings to the nickel oxyhydroxide electroactive materials in the electrochemical, morphological and structural aspects.

First of all, I would like to thank my thesis supervisor Prof. Dr. Mustafa Ürgen for providing me great opportunities, sharing his great knowledge with me, teaching me about the scientific approaches and the way of thinking while doing science. His willingness to learn and teach will be something that will inspire me for the rest of my academic career. I will carry the honor of being his student for my whole life.

Secondly, I thank Burçak AVCI, Çağatay YELKARASI, Erkan KAÇAR and Seyhan ATİK for their guidance about experimental setups and their support during my thesis work. Their great patience and willingness to help greatly influenced me during my master's studies.

I thank to Prof. Dr. Gültekin Göller and Hüseyin SEZER due to their help for my morphological investigations by using SEM.

I am grateful to Melike GÜNERTÜRK for her continuous support, patience and caring. She provided me the strength to complete my studies and picked me up whenever I was down.

Finally, I would like to thank my mother and father for all of their sacrifices, unconditional support and love. Their support in every situation gave me the freedom and confidence to pursue my passions.

June 2020

Berke KARAMAN
Metallurgical and Materials Engineer

TABLE OF CONTENTS

Page

ABBREVIATIONS

CP	**:** Chronopotentiometry
CV	**:** Cycling voltammetry
CNT	**:** Carbon nanotubes
EDLC	**:** Electrical double layer capacitor
EIS	**:** Electrochemical impedance spectroscopy
SEM	**:** Scanning electron microscopy
PANI	**:** Polyaniline
PPy	**:** Polypyrole
XRD	**:** X-Ray Diffractometry

SYMBOLS

C	**:** Capacitance
Rs	**:** Solution resistance
Rct	**:** Charge transfer resistance
A	**:** Geometric surface area
i	**:** Current
Va	**:** Anodic potential
Vc	**:** Cathodic potential
Δt	**:** Discharge time
V	**:** Potential

LIST OF TABLES

Page

LIST OF FIGURES

Page

CONTRIBUTION OF MXENE COATINGS TO THE PERFORMANCE OF NICKEL BASED ELECTROACTIVE MATERIALS

SUMMARY

Energy storage devices are gaining more and more attention due to the increasing need for more and faster energy storage. Energy storage devices can work with two different kinds of storage mechanisms in general which are electrical double layer and faradaic reactions. Electrical double layer mechanism works with electrostatic interactions within the oppositely charged ions while faradaic reactions are based on charge transfer between the particles. When compared to other energy storage devices like batteries and fuel cells, supercapacitors forefront with their high power density and high cycling stability however, their energy density is much lower than other energy storage devices. Therefore, new studies aim to increase energy density while keeping high power density and high cycling stability. Three traditional material types are used as supercapacitor electrodes which are carbon based materials, metal oxides and polymers. Carbon based materials' charge storge mechanism is solely based on double layer mechanism which provides high power density but very low energy density. Polymers provide high energy density however, their shrinkage and swelling during charge storage degrades their performance. Meanwhile, metal oxides energy storage mechanism is based on faradaic reactions which provide high energy density but their cycling stability is relatively low due to possible phase transformations. Nickel hydroxides are one of these materials that are used in supercapacitor electrodes. Their ability to possess high specific capacitance, ease of production and environmentally friendly nature brings attention. Nickel hydroxides have three different phases which are alpha beta and gamma. Alpha phase provides better electrochemical performance while beta phase has lower capacitances and gamma phase is considered the intermediate phase in cycling. However, alpha phase when cycled in KOH electrolyte, transforms into beta phase due to aging which results in poor cycling stability. In addition to three traditional electrode materials types, a new type of electrode materials emerges as 2 dimensional materials including graphene, phosphorene and mxenes. Mxenes are forefront with their high capacitance that could already reach to the highest capacitance obtained by metal oxides which is 1500 Fcm^{-3}. However, none of these materials are enough the met required needs therefore combinations of these materials are used in order to combine the best aspects of these materials and close the deficts of each other.

In this thesis, $Ti_3C_2T_x$ mxene is produced by LiF+HCl method and coated with electrophoretic deposition on the NiOOH that is produced with anodic oxidation. Production methods are specially selected as binder-free methods in order to eliminate using binders that would reduce the performance of the electrode. Parameters of production of mxenes are optimized as 12M LiF+9M HCl at 45ºC for 24 hours while NiOOH are produced in KOH at 200ºC for 30 minutes with anodic oxidation method. Electrophoretic deposition parameters set at 50 V for 5 minutes in 50 ml Acetone with the addition of 0.003g I_2. In each production step, binder-free production methods are preferred in order to enhance the electron transfer between electroactive materials and

current collector. In order to see the direct effect of the combination of NiOOH and $Ti_3C_2T_x$, all NiOOH, $Ti_3C_2T_x$ and composite NiOOH/$Ti_3C_2T_x$ are produced as separate electrodes and characterized before and after 1000 cycling to observe morphological, structural and electrochemcial changes as well as the performance of these electrodes. As a result, capacitance of the composite electrode is almost twice (1.91 F/cm^2) of the NiOOH electrode (1.15 F/cm^2) and four times of the mxene electrode (0.41 F/cm^2). However, the addition of mxene coating on the NiOOH was not impactful in the capacity retention aspect as both NiOOH and composite electrode lost around 60% of its capacitance after 1000 cycles. After structural and morphological characterizations, it is observed that mxene coating could not prevent the phase transformation of the NiOOH from gamma to beta and also, mxenes are oxidized after 1000 cycles. Even though flowerlike morphology of the NiOOH is preserved, the flaky structure of mxenes diminishes after 1000 cycles in both composite electrode and bare mxene electrode which can be a result of the oxidation. Further, performance boost of the composite electrode is inspected with electrochemical techniques. Electrochemical impedance spectroscopy has been used in order to further evaulation of electrochemical properties. Solution resistance of composite electrode (0.329 Ω) found to be lower than both mxene (0.474 Ω) and NiOOH electrode (0.642 Ω) . Meanwhile, Nyquist plots clearly show that diffusion properties of the composite electrode is enhanced as slope of the vertical line on the low frequency region is the highest. Rate capabilities which is greatly affected by the diffusion capabilities, shows that while NiOOH electrode can keep 12% of its capacitance when scan rate is increased from 1mv/s to 100 mv/s, mxene electrode can keep 24% of its capacitance which is reflected as 16% in the composite electrode. Meanwhile, electrodes are characterized by the scan rate and peak current relations and observed that all three electrodes reaction mechanisms are heavily dependent on the diffusion properties. It is concluded that surface area increase and the structure of the mxenes significantly improve the electrode's diffusion properties and result in high capacitance and high rate capability. As a result, it is observed that mxene deposition on NiOOH flowerlike structures dramatically increases the surface area and enhances diffusion properties, which reflects to the performance of the electrode.

MXENE KAPLAMALARIN NİKEL BAZLI ELEKTROAKTİF MALZEMELERİN PERFORMANSINA ETKİSİ

ÖZET

Enerji depolama aygıtlarına duyulan ihtiyaç gün geçtikçe artmaktadır. Daha hızlı şarj olabilen ve daha fazla enerji saklama kapasitesine sahip olan enerji depolama aygıtları üretmek için araştırmalar gün geçtikçe artmaktadır. Enerji depolama aygıtları genel olarak 2 farklı mekanizma ile çalışabilmektedir. İlk olarak, elektriksel çift tabaka mekanizması farklı yükteki iyonların elektrostatik olarak etkileşmesi ile enerji depolayabilirken, faradaik enerji depolama mekanizması elektrotlardaki redoks reaksiyonlarına bağlı yük değişimleriyle çalışır. Bu bağlamda, süperkapasitörler hızlı şarj deşarj olabilmeleri ve yüksek çevrimsel stabiliteleriyle diğer enerji depolama aygıtlarından öne çıkmaktadır. Süperkapasitör malzemeleri olarak genelde üç farklı malzeme çeşidi bulunmaktadır; karbon bazlı malzemeler, metal oksitler ve polimerler. Karbon bazlı malzemelerin enerji depolama mekanizmaları çift tabaka mekanizmasına bağlıdır ve faradaik reaksiyonları içermez. Dolayısıyla hızlıca şarj-deşarj olabilirler ve çevrimsel ömürleri uzundur. Ancak karbon bazlı malzemelerin düşük kapasiteleri, kullanım olanaklarını sınırlamaktadır. Polimerler ise faradaik reaksiyonlarla enerji depolarken, yüksek kapasitelerine rağmen şarj deşarj sırasındaki şişme ve büzüşmeleri sebebiyle mekanik olarak bozundukları için çevirmsel ömürleri düşüktür. Polimerlerin bu konudaki en avantajlı özelliği ise diğer malzemelerin ağırlıklı yüzeylerinde gerçekleşen reaksiyonlarına karşın, polimerlerde bu reaksiyonlar polimerlerin fiberli yapıları sayesinde malzemenin hacminde gerçekleşir. Metal oksitler ise faradaik reaksiyonlarla enerji depolamalarıyla birlikte yüksek kapasiteleri, kolayca sentezlenebilmeleri sebebiyle tercih edilen bir malzeme çeşididir. Ancak genel olarak kimyasal kararlılıkları yüksek olmasına rağmen metal oksitlerdeki faz dönüşümleri çevrimsel stabilitelerini düşürebilir. Dolayısıyla metal oksit malzemeler hakkındaki araştırmalar kapasiteyi arttırmanın yanı sıra, çevrimsel stabilitenin de arttırılmasına odaklanmıştır. Metal oksit malzemeler arasında, nikel oksit/hidroksitler yüksek kapasite değerleri, çeşitli üretim yöntemleri olması ve çevre dostu olmaları sebebiyle tercih edilmiştir. Nikel hidroksitlerin temelde alfa beta ve gamma olarak 3 ayrı fazı bulunmaktadır. Bu fazlar arasında alfa nikel hidroksitlerin elektrokimyasal özelliklerinin daha iyi olması sebebiyle yüksek kapasitans değerlerine ulaşabilirken potasyum hidroksit elektolitleri içinde yaşlanma sebebiyle faz dönüşümüne uğrayıp beta nikel hidroksite dönüşmektedir. Gama oksinikelhidroksit ise alfa fazlarının şarj deşarj sırasında dönüştüğü ara faz halidir. Nikel hidroksitlerin kapasitesinin yüksek olmasına rağmen yaşlanma sebebiyle faz dönüşümüne uğraması kapasitesini büyük oranda etkileyip kullanımını sınırlandırmıştır. Son olarak, üç geleneksel elektrot malzemesi türüne ek olarak iki boyutlu malzemeler keşfedilmiştir. Bu malzeme türleri diğer malzeme türlerinden farklı eşsiz özelliklere sahiplerdir ve grafen, fosforen ve mxene gibi mazlemeleri içinde barındırmaktadır. Bu malzeme türlerinden olan mxene MAX fazı malzemelerdeki “A” elementinin selektif olarak giderilmesiyle oluşan iki

boyutlu katmanlı yapılardır. Enerji depolama mekanizması yapısındaki geçiş metalinin redoks reaksiyonlarından yararlanırken yapısındaki karbon tabakası elektronların hızlıca iletilmesini sağlamaktadır. Mxeneler şimdiden metal oksitlerin ulaştığı en yüksek kapasitelerden biri olan 1500 Fcm^{-3}'e erişse de enerji ihtiyacını karşılamada yeterli değildir. Dolayısıyla yukarıda belirtilen malzeme türlerinin tek başına kullanıldığında enerji ihtiyacını karşılayamaması sebebiyle bu malzemelerin birlikte kullanıldığı kompozitler üretilmiştir. Bu kompozitlerde amaç malzemelerin birbirinin eksik yönlerini kapatarak toplamda yüksek performanslı bir süperkapasitör elektrodu geliştirmektir.

Bu çalışmada $Ti_3C_2T_x$ mxene, LiF+HCl methoduyla üretilmiş ve elektroforetik biriktirme methoduyla, anodik oksitleme methoduyla üretilmiş NiOOH üzerine kaplanmıştır. Bu methodlar bağlayıcıların performansı büyük oranda etkilemesi dolayısıyla, bağlayıcı içermeyen methodlar olarak seçilmiş. Mxene üretim methodu ve elektroforetik biriktirme methodunun paramtere optimizasyonu yapılmıştır. Mxene üretimi, 7.5M LiF+9M HCl çözeltide oda sıcaklığında denenmiş ve yeterli sonuca ulaşılamamıştır. Daha sonra 12M LiF+9M çözeltide ve oda sıcaklığında gerçekleştirilmiş ve MAX fazının büyük ölçüde mxene yapısına dönüştüğü gözlemlenmiştir. Sıcaklığın arttırılmasıyla MAX fazının neredeyse tamamen mxene yapısına dönüştüğü gözlemlenmiştir. Sonuç olarak mxene üretiminde en iyi verim 12M LiF+9M HCl çözeltisinde ve 45ºC derecede alınmıştır. Elektroforetik biriktirme methodunda ise, elektrodlara 50V potansiyel 5 dakika boyunca 0.003g I_2 + 50 ml aseton+0.5g $Ti_3C_2T_x$ elektrolitinde uygulanmıştır ve kaplama katotta elde edilmiştir.

Her üretim methoduna bağlayıcı içermeyen üretim yöntemleri tercih edilerek malzemenin direkt altlık üzerine kaplanması, dolayısıyla da elektron taşınımını kolaylaştırarak daha iyi performans elde etmek amaçlanmıştır. Ayrıca bağlayıcıdan kaynaklanabilecek sorunların ve çevrimsel stabilite düşüşünün de önüne geçilmek istenmiştir. Çalışma kapsamında, mxene kaplamaların NiOOH elektroda katkısını sağlıklı bir şekilde gözlemleyebilmek için NiOOH, $Ti_3C_2T_x$ ve NiOOH/$Ti_3C_2T_x$ olarak üç farklı elektrod üretilip üçü de morfolojik, yapısal ve elektrokimyasal performans olarak karakterize edilmiştir. Karakterizasyon aşamaları 1000 çevrimden önce ve sonra tekrarlanarak elektrodların çevrim performası gözlemlenmiştir. Sonuç olarak 20 mv/s tarama hızıyla karakterize edildiklerinde, kompozit elektrodun (1.91 F/cm^2) NiOOH elektrodun (1.15 F/cm^2) yaklaşık iki, mxene elektrodun(0.41 F/cm^2) yaklaşık beş katı kapasiteye sahip olduğu görülmüştür. Ancak kompozit elektrodun NiOOH elektroda benzer bir kapasite düşüşü göstermesi sebebiyle, mxene kaplamanın çevrim direncine etkisi olmadığı gözlemlenmiştir. NiOOH ve kompozit elektrotların ikisi de kapasitesinin yaklaşık %60'ını 1000 çevrim sonucunda kaybetmişlerdir. Yapısal ve morfolojik karakterizasyonların sonucunda mxene kaplamanın nikel oksihidroksitin faz dönüşümünü engelleyemediği, kompozit elektrodtaki nikel oksihidroksitin de beta fazına dönüştüğü görülmüştür. NiOOH çiçeksi yapısını korurken 1000 çevrim sonucunda mxene'in ise pulsu yapısını hem kompozitte hem de tek başına bulunduğu elektrodta kaybederek yüzey alanının azaldığı daha kompakt bir morfolojiye dönüştüğü görülmüştür. Morfolojik değişimin nedeni RAMAN ile araştırılmış ve yapıdaki karbon bağları gözlemlenmiştir. Buna göre, yapıdaki defektif karbonun arttığı gözlemlenmiş bunun sebebinin titanyum atomlarının oksijenle bağ yapıp geriye defektif karbonu bıraktığı anlaşılmıştır. Dolayısıyla, mxenelerin karbon bağlarının RAMAN ile araştırılması sonucu mxenelerin 1000 çevrim sonucunda oksitlendiği anlaşılmıştır. Elektrokimyasal empedans spektroskopisiyle elektrodların elektrokimyasal özellikleri gözlemlenmiş, sonuç olarak kompozit elektrodun çözelti

direncinin (0.329 Ω) diğer iki elektrodtan (mxene 0.474 Ω, NiOOH 0.642 Ω) düşük olduğu gözlemlenmiştir. Ayrıca, nyquist diyagramları karşılaştırıldığında, kompozit elektrodun düşük frekans bölgesinde en dik eğime sahip olduğu dolayısıyla da en iyi difüzyon özelliklerine sahip olduğu görülmüştür. Dolayısıyla, kompozit elektrodun artan performansının sebeplerinden birinin kompozit elektrodun üstün elektrokimyasal özellikleri olabileceği anlaşılmıştır. Daha sonra değişen tarama hızlarına elektrodların verdiği tepkilerin ölçülmesi amacıyla çeşitli tarama hızlarında elektrodların kapasiteleri hesaplanmıştır. Tarama hızlarının elektrod kapasitesine etkisi malzemelerin difüzyon özellikleriyle ilintili olup, yüksek difüzyon özelliklerine sahip malzemelerin tarama hızı değişimine daha çok tolerans göstermesi beklenmektedir. Sonuç olarak, tarama hızı 1 mv/s'den 100 mv/s'e çıkartıldığında NiOOH elektrodun kapasitesinin %12'sini, mxene elektrodun %24'ünü kompozit elektrodun ise %16'sını koruyabilidği görülmüştür. Dolayısıyla, mxene'lerin iyon ve elektron difüzyonu özelliklerinin yüksek olduğu gözlemlenmiş, bu özelliklerini kompozit elektroda da taşıdığı anlaşılmıştır. Akım-tarama hızı ilişkisi de elektrodlar için kurulmuş, üç elektrodun da çalışma mekanizmasının difüzyon ağırlıklı olduğu bulunmuştur.

Sonuç olarak, tüm elektrodlar bağlayıcı içermeyen üretim yöntemleriyle üretilmiştir. Üretilen elektrodlar mxenelerin nikel oksihidrokist elektroda katkısını incelemek amacıyla morfolojileri, yapıları ve performansları gözlemlenmiştir. Sonuç olarak, mxene kaplamaların elektrod yüzey alanını arttırması ve kendi katmanlı yapısı sayesinde kompozit elektrodun difüzyon özelliklerine büyük oranda katkıda bulunması sebebiyle kapasiteyi büyük oranda arttırdığı gözlemlenmiştir. Arttırılan yüzey alanının ve yükselen difüzyon özelliklerinin performansa etkisi açık bir şekilde görülmekteyken bu özelliklerin çevirmsel stabilitiye etkisi gözlemlenmemiştir.

1. INTRODUCTION

Energy storage is one of the most important issues of the energy industry as demand for storage increases day by day. Energy storage devices help the community by storing the produced energy to use it when it is needed. Available energy as long as it can be stored and used when needed, even if the production of energy is increased. Therefore the researches are focused on environmentally friendly, cost-efficient and high capacity energy storage devices.

There are many energy storage devices that are used in daily life; batteries, fuel cells, supercapacitors. Among those, supercapacitors are prominent with their high power density and high cycle life compared to fuel cells and batteries [1]. However, the lower energy density of supercapacitors compared to other energy storage devices is their main disadvantage. Researches are now focused on increasing the energy density of the supercapacitors without sacrificing any power density and cycle life. So far, there are various electrode materials that are used as electroactive materials in supercapacitor electrodes. Metal oxides, carbon based materials, polymers and 2D materials are the main types of electroactive materials. Carbon based materials are highly abundant materials that have high conductivity. Their charge storage mechanism is based on the double layer phenomenon and exhibits very high cycle life and conductivity. However, the capacity that can be acquired from these materials limited [2]. Conductive polymers is another group of materials that work under the same principle with increasing popularity. However, because of mechanical and chemical degradation during cycling, their stability is relatively low [3]. For the moment metal oxides are the group of materials that exhibit high capacity as a result of the charge transfer reactions during cycling known as faradaic reactions. However, low cycle life is the main drawback of metal oxide electroactive materials therefore the researches are focused on increasing the stability of metal oxides. Nickel hydroxides are one of these materials that are frequently used due to their high capacitance, ease of production and enivronmental friendly nature. However, their degradation during cycling reduces the performance of nickel hydroxide materials therefore, researches are focused to increase the stability of the nickel hydroxide as well as increasing the capacitance.

In this project, nickel-based electroactive materials are selected as one of the composite components because of its high theoretical capacitance and ease of controllable oxidation; therefore, it can be produced directly on the substrate surface.

Supercapacitor electrode material types can vary not only with the elements used in it, but also with the morphology and structure. The new type of the electroactive materials known as 2D materials are now seen as the most promising materials for energy storage devices because of their high conductivity, high surface area and high cycle life. Among those materials, transition metal carbides, known as mxenes are recently discovered in 2011 by Gogotsi and his group. These materials are prominent with their layered structure that promotes the surface area which results in high capacity. The metallic conductivity of the mxenes films provides electrons to all electrochemically active sites and transition metal redox reactions provide pseudocapacitance which all results in high capacity and high power density. The capacity of mxenes already caught up with the highest capacity obtained with metal oxides which is 900 Fcm^{-3}. However, none of these materials can meet the required capacity alone. Therefore, the combination of these materials are used to promote the best aspects of the materials in composite and reduce negative aspects by the synergetic effect between them.

The main objective of this work is to improve the performance of the nickel oxyhydroxide electrodes by introducing mxene into their structures. One of the originalities of the study is to produce a composite without using binders. Previous studies on combining nickel oxide based pseudo capacitor materials with mxene are limited [4], [5]. In both of these studies mxene powders are mixed with polymers and carbon black to produce a paste that is applied on conducting surfaces. We did not come across any studies for the binder-free production of these composites.

In order to make an healthy comparison, and along with NiOOH/$Ti_3C_2T_x$ (NHM) composite electrodes pure nickel oxhydroxide electrode (NH), pure $Ti_3C_2T_x$ (mxene) electrode are also produced. We have selected binder free production methods for each step of the production of the electrodes, to enhance the performance. Therefore, nickel oxyhydroxides are produced with anodic oxidation method while mxenes are deposited with electrophoretic deposition method. Optimization of production parameters of $Ti_3C_2T_x$ mxene has been conducted for various molarities of LiF+HCl method as well as reaction temperature. Meanwhile, optimization of electrophoretic deposition method also conducted in order to eliminate any bubble formation

to obtain homogeneous and compact coating without damaging the nickel oxyhydroxide morphology . Produced electrodes are subjected to cycling for 1000 cycles in 6M KOH electrolyte and further characterizations has been conducted with RAMAN, EIS, SEM before and after 1000 cycles in order to observe changes in the structure, electrochemical properties and morphology. Meanwhile, charge-discharge tests and scan rate-current relations conducted in order to obtain more information about the electrochemical characteristics of these electrode materials.

2. LITERATURE REVIEW

2.1. Energy Storage Mechanisms

Generally, there are two mechanisms for storing energy; electric double layer capacitance and faradaic reactions. Electric double layer capacitance uses the electrostatic interaction between oppositely charged ions in the electrolyte and surface of the electrodes (Figure 2.1) [6]. This effect creates the layers at the interface of electrolyte and electrode which is called as double-layer. The relation that is used to calculate the capacitance is the following:

$$C = \varepsilon \frac{A}{d} \tag{1}$$

Where ε is permittivity, A is the surface area of the electrode and d is the distance between plates. By looking at equation (1), in order to increase the capacitance, the distance between plates should be decreased or the surface area of the electrode should be increased. However, the distance between plates practically cannot be set at some microns or nanometers. Therefore, using an electrolyte between plates rather than air is the main difference between supercapacitors and conventional capacitors. Electrolyte minimizes the distance between

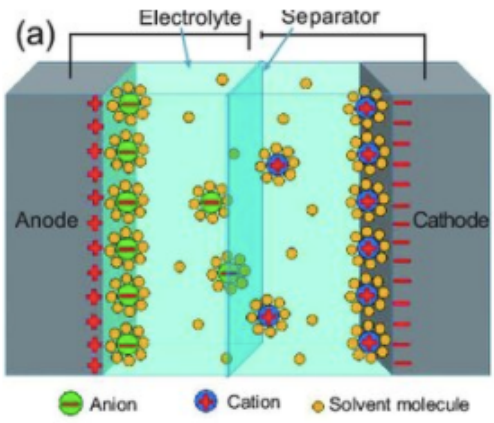

Figure 2.1 Schematic represatation of electrical double layer capacitor. [6]

opposite charges and as a result, supercapacitors can accomplish multitudes of the capacities of conventional capacitors. After this is accomplished, only thing that is left in the equation is A which is the surface area of the electrode. Therefore, to increase stored energy with this mechanism, the main route is to increase the surface area of the electrode thus increasing the available surface for ion adsorption.

The second mechanism is the faradaic reactions, which involve the charge transfer between the electrolyte and electrode during charging and discharging (Figure 2.2) [7]. This is also known as the psuedocapacitance, which includes redox reactions and intercalation processes. In faradaic reactions, there are no chemical reactions between the electrolyte and the electrode, only charge transfer occurs. The metal oxides switch between its oxidation states and provide the faradaic reactions.

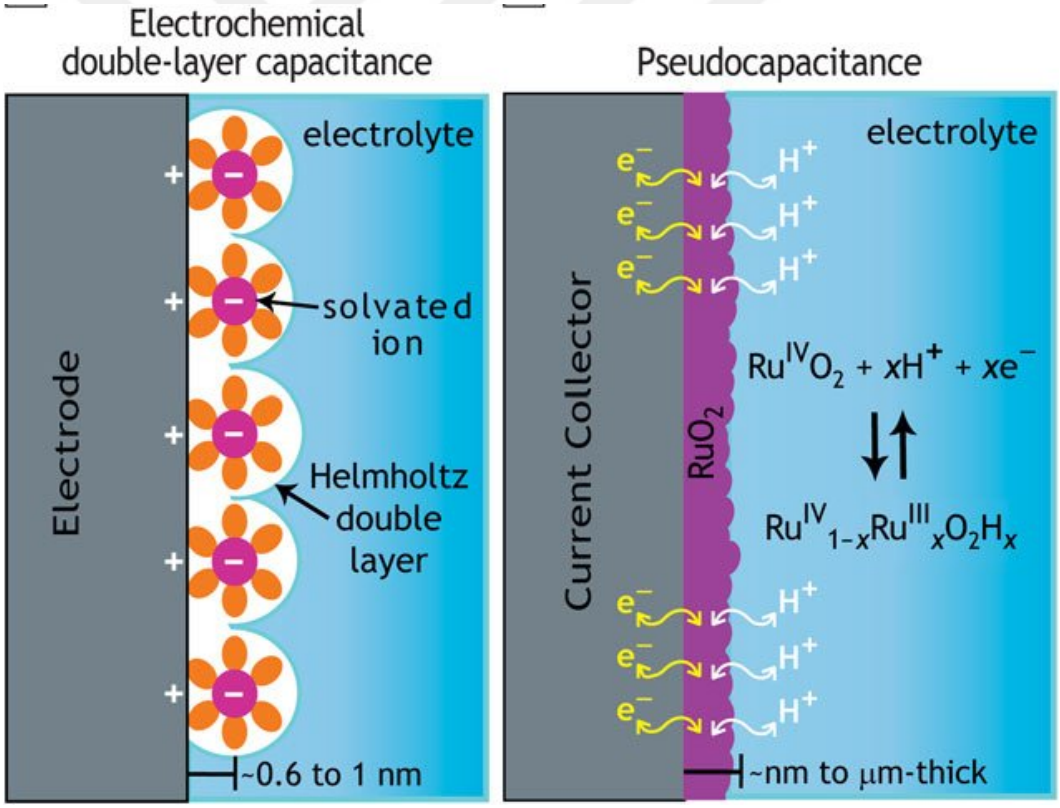

Figure 2.2. Representation of working mechansims of electrochemical double layer capacitance and pseudocapacitance. [7]

2.2. Energy Storage Devices

There are various types of energy storage devices that includes supercapacitors, batteries and fuel cells. Those devices are divided by their working mechanisms as well as characteristic storage procedures. Each type of storage device has its advantage and disadvantage. In order to classify the needs, spesific power which is watt per kilograms and spesific energy that is watt hour per kilogram is used. [8]

Fuel cells have the highest spesific energy namely the amount of energy that could be stored per weight. However, their specific power, which can roughly be described as the charging time, is relatively lower than other devices. Capacitors are in the right bottom of the graph thus they can be charged very quickly but their capacity is much lower than other storage devices (Figure 2.3). Li-ion batteries are occupying the intermediate position between fuel cells spesific energy and capacitors.

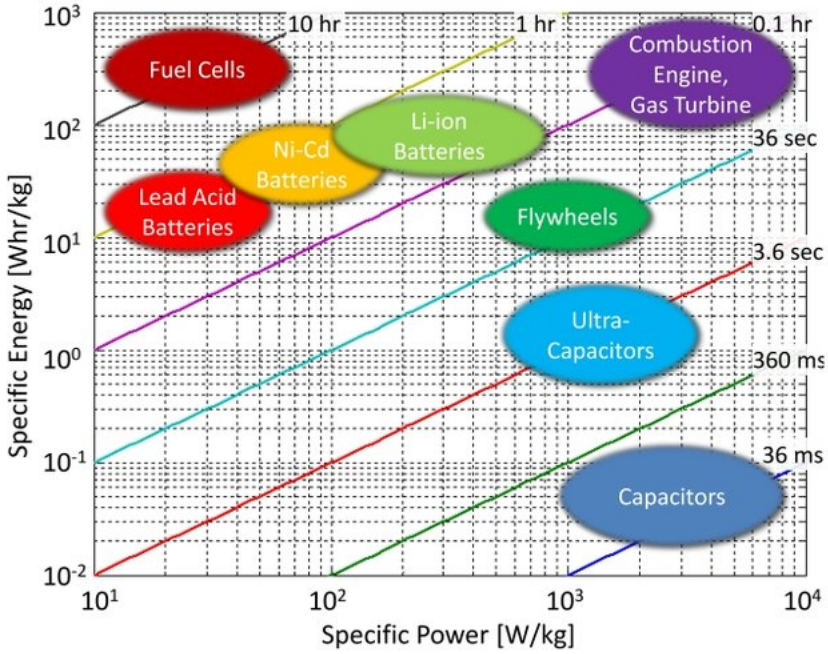

Figure 2.3 Ragone plot of energy storge devices. [8]

Eventually, the ultimate goal of the energy storage device research is to obtain high capacity, fast charging device.

2.2.1. Supercapacitors

Supercapacitors principally work the same way the conventional capacitors work. However, the electrolyte between two electrodes reduces the “d” to the nanometer level as electrolyte behaves like an electrode thus brings the capacity of the capacitors to the much higher levels. In 1957, the first patent for the supercapacitors is issued by H.Becker . Although the history of supercapacitors dates back to 1966, [9] their potential as charge stroage devices became appreciated after the pioneering studies of B. Conway on the fundamentals of supercapacitor materials.

Supercapacitors are superior to the other energy storage devices with their outstanding capacity retention and high power density. These properties are result of their working mechanisms which are double layer capacitance and/or faradaic reactions. Even though the distinction between other energy storage devices are appearent, the differences between batteries and pseudocapacitors are still in discussion to this day.

2.2.2. Battery or pseudocapacitor?

Distingushing of electric double layer capacitors from batteries and pseudocapacitors is straight-forward. They provide great cycling stability and high power density that is represented with rectangular cyclic voltammogram. Since double-layer mechanism does not involve any diffusion, charge separation is instant under an external field therefore dV/dt is constant. However, the distinction between pseudocapacitors and batteries is more complicated than that as both devices involve faradaic reactions and their working mechanism is similar. There are various discussions and suggestions about the differences between batteries and pseudocapacitors. The first consideration is phase transformation. During cycling, phase transformation does not occur in the pseudocapacitors. Ions are either adsorbed on the electrodes surface and faradaic charge transfer occurs or ions intercalate into the structure of the electrode and faradaic charge transfer occurs. However, in battery material case, charging is followed by a phase transformation of electrode material. This phase transformation is characterized as distinct peaks on the cycling voltammogram. Meanwhile, for the pseudocapactive materials, a rectangular shape is observed on the cycling voltammogram. This behavior represents the reversible changes in the oxidation state of the material. Also, according to Conway’s definition, capacitances of the supercapacitor electrodes should be constant over

the whole potential window [10]. Another concept for the distinguishment is the intrinsic kinetics of the faradaic reactions. Scan rate dependence of the electrodes brings insight into the intrinsic kinetics of the electrode materials. In battery electrodes, there is a $i \sim v^{1/2}$ relationship that is indicative of semi-infinite diffusion while in supercapacitor scan rate dependence for current is linear as i~v.[11]

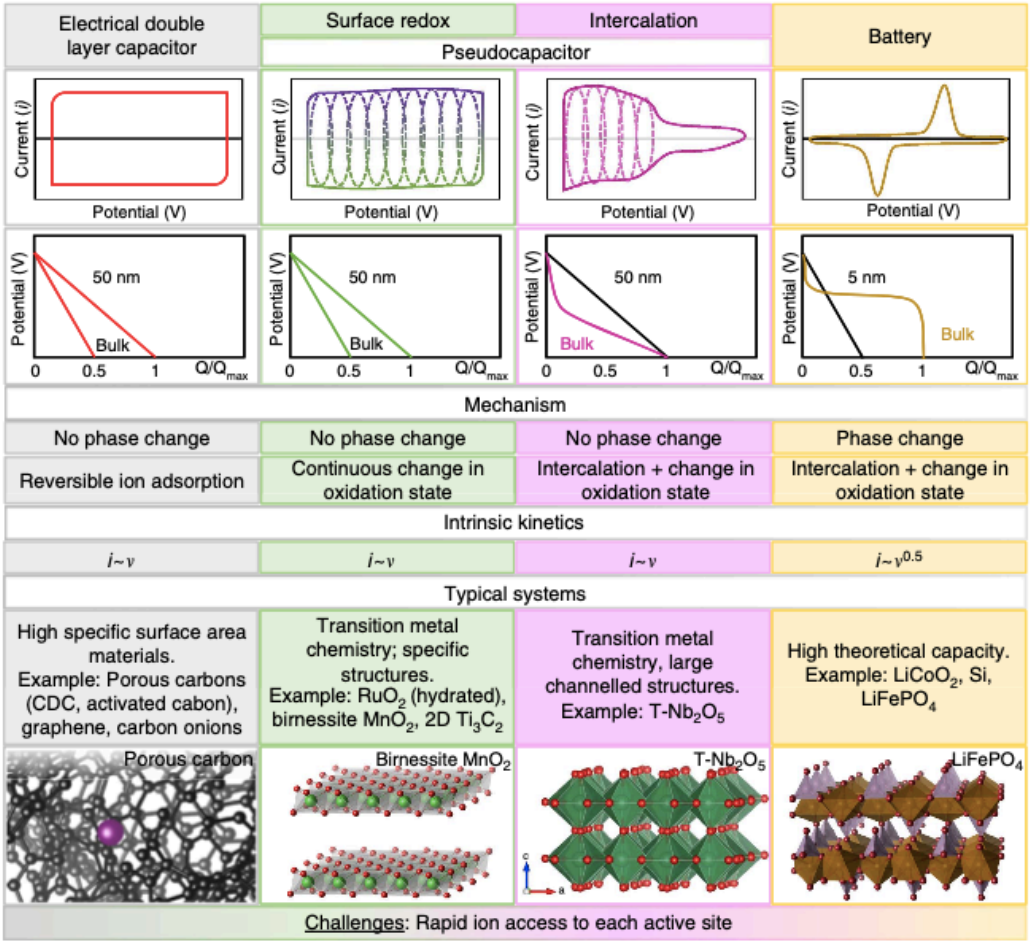

Figure 2.4. Summary of the energy storage mechansims. [11]

However, if the said battery materials are prepared in nanoscales, they may act as pseudocapacitive material and do not show any phase transformations. This is due to increase in surface area and decrease in the diffusion distances. Therefore, strain that occurs as a result of ion insertion in the bulk battery material does not take place and phase transformation can be avoided. These kind of materials are known as extrinsic pseudocapacitive materials while materials following the pseudocapacitive characteristics in broad range of particle sizes and

morphologies known as intrinsic pseudocapacitive materials [12]. Therefore, by modifying the particle sizes of a battery-type material, pseudocapacitive characteristics can be observed like triangular shapes in charge-discharge curves (Figure 2.5).

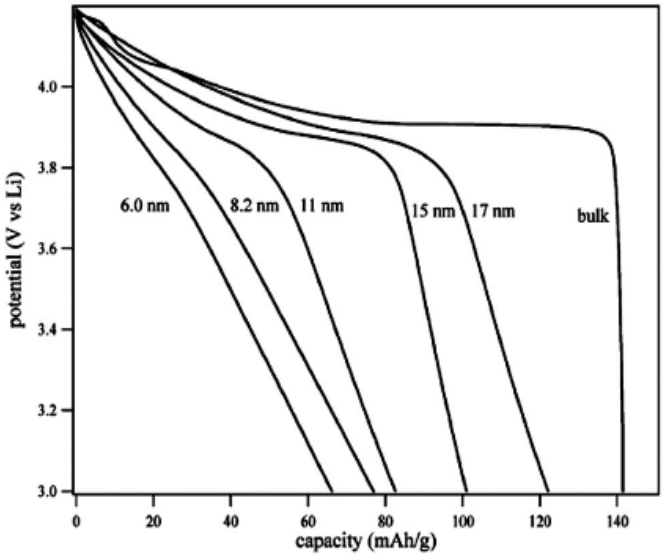

Figure 2.5. Representetive charge-discharge curves. [12]

However, these materials cannot be represented as high energy density supercapacitors if they are tested with a low rate because this is against the notion of supercapacitors having high power densities. Proposed parameters for required tests is to use fully charged in 1 min with the rate of 60C [13].

2.2.3. Performance tests for energy storage devices

There are various types of test to determine the performances of supercapacitors. According to tests; capacity, capacity retention, resistances and working mechanisms can be determined.

2.2.3.1. Cycling voltammetry

Cycling voltammetry (CV) is one of the most popular characterization methods for energy storage devices. The linearly sweeped potential between working electrode and reference electrode causes an oxidation or reduction reaction in the working electrode thus a charge transfer occurs. This movement of electrons generates an electrical current and the generated current is measured. A typical cyclic voltammogram is drawn according to potential vs currents.

Cylic voltammogram (Figure 2.6) gives information about the characteristics of devices such as peak currents, potential ranges, capacitance, reversibiltiy of the reactions and oxidation and reduction potentials.

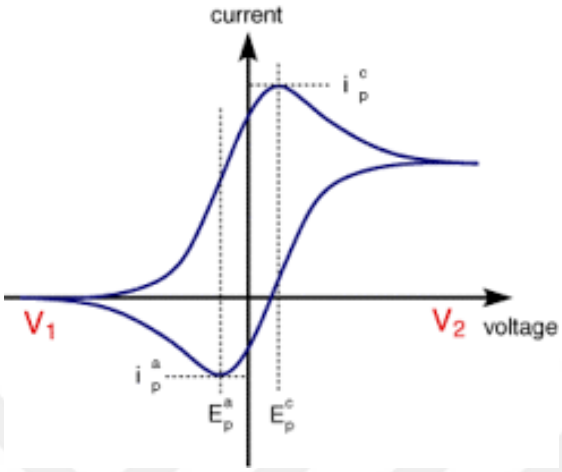

Figure 2.6. Representetive cycling voltammogram graph.

Capacity of an electrode can be calculated by the following formula by using cycling voltammetry;

$$C = \frac{(\int_{Va}^{Vc} i(V)dV)}{V \times A \times (Va - Vc)} \quad (2)$$

$\int_{Va}^{Vc} i(V)dV$ = The area under CV curve

C= Capacitance(F/cm^2)

V= scan rate (mV/s)

A= the area of the electrode in the electrolyte (cm^2)

Va-Vc= Potential range Va as anodic potential and Vc is cathodic potential

i = current (mA)

2.2.3.2. Chronopotensiometry (Charge-Discharge)

Charge-Discharge test is used to determine the behavior, capacitance and cycle life of the electrodes. In this test, a constant charging current is applied to the electrode and responses in potential according to reference electrode is recorded. After the electrode is fully charged, discharging starts with a constant current and the discharge time is recorded. Capacitance can be calculated with following equation:

$$C = \frac{I \times \Delta t}{s \times \Delta V} \tag{3}$$

C= Capacitance(F/cm^2)

I= Charging/Discharging current

Δt= Discharge time

ΔV= Potential range

S= Surface area of the electrode

2.2.3.3. Electrochemical impedance spectroscopy

Electrochemical impedance spectroscopy is one of the most used characterization techniques for energy storage devices. It gives detailed information about reaction kinetics in the cell. AC is applied to the electrode in the open circuit potential with a wide range of frequency and response of the cell is recorded. In high frequencies, equivalent series resistance and inductance of the cell is characterized while high-mid frequencies electrode reactions are inspected and in low frequencies diffusion dominates the spectra. For the energy storage applications, electrochemical impedance gives crucial informations like internal resistance, charge transfer resistance and capacitances.

2.3. Supercapacitor Electrode Materials

Supercapacitor electrodes can be manufactured from a variety of materials. Carbon-based materials, metal oxide based materials, conductive polymers and two dimentional materials are the main types of supercapacitor electrode materials.

2.3.1. Carbon-based electrode materials

Carbon based materials are one of the most popular electrode materials due to their abudance in nature, high conductivity and high surface area. Activated carbon, nanoporous carbon and carbon nanotubes are the most popular materials for supercapacitor electrode applications. Energy storage mechanism of carbon based electrodes is based on electrical double layer and they do not show any faradaic behavior in their undoped state. Carbon based materials also used as an additive to the electrodes in order to increase the conductivity of the electrode.

Graphite is the basic form of carbon based electrodes with its hexagonal layered structure that includes sp^2 bonds. They are widely used in Li-ion batteries as anodes and as additives. Graphite generally used as in the form of porous carbons which includes activated carbons and nanoporous carbons.

Carbon nanotubes are the tubes in nanometer level that are made of carbon. CNTs are classified by the number of walls as “single walled carbon nanotubes” or “multi wall carbon nanotubes”. The long tube structure provides a good electronic transport property as there is no electronic scattering. The entanglement of CNTs provides a porous structure that boosts the ion diffusion which is a crucial part of the charging-discharging phenomena [14].

2.3.2. Metal oxide based electrode materials

Transition metal oxides are one of the most popular supercapacitor electrode materials because of their high capacitance, diverse morphologies and high surface area. However, their capacity retention property is relatively low when compared to the carbon based materials. TMOs energy storage mechanism is based both on faradaic reactions and double layer capacitance. Namely, RuO_2, $Ni(OH)_2$, MnO_2, Fe_2O_3, V_2O_5 are the most popular TMOs for supercapacitor electrode applications. During charging and discharging, transition metal cycles between its oxidation states and provides the charge transfer between electrolyte and the electrode. These reactions can be observed in cycling voltammogram as peaks.

Among these transition metal oxides, nickel based electrode materials become prominent with their high capacitance, ease of production and environmental friendly nature.

2.3.3. Conductive polymer based electrode materials

Conductive polymers provides high capacitance and high electrical conductivity compared to the carbon based materials. Polyaniline (PANI), poli-(3,4-etilendioksitiyofen) (PEDOT) and polypyrole (PPy) are the most popular conductive polymers in supercapacitor electrodes. Energy storage mechanism of conductive polymers is mainly based on faradaic reactions.

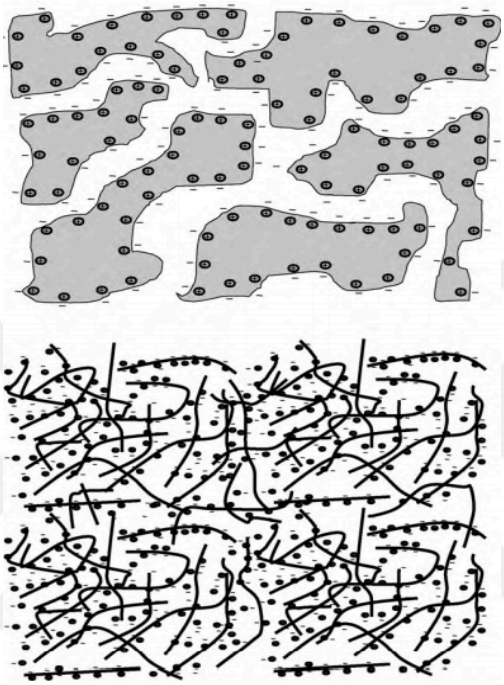

Figure 2.7. Comparison of charging of carbon and conducting polymers. [15]

One of the main advantages of conductive polymers is that faradaic reaction that takes place between entire bulk material rather than the surface (Figure 2.7) [15]. Oxidation occurs with ions that are transferred to the polymer backbone and they are released back into electrolyte when oxidation takes place [16]. This is also known as doping and dedoping. Since there is no structural change involved like phase changes, the charging-discharging of conductive polymers are highly reversible [17]. However, their working potential range is rather limited because they can get degraded in more positive potentials and they can turn into insulating state when potentials are more negative. Becasue of their low capactiy retention properties conducting polymers are generally used with other types of electrode materials such as transition metal oxides and carbon based materials. Polyaniline and carbon nanotubes are used

together as a supercapacitor electrode by Gupta et al. and obtained promising results as a spesific capacitance of 485 Fg^{-1} with a good cyclability [18]. Manganase oxide and polyaniline combined as a supercapacitor electrode by Prasad and Miura and obtained high spesific capacatiance as 715 Fg^{-1} .[19]

2.3.4. 2D Materials

Two dimentional materials are relatively new types of materials. First synthesis was the nobel winning graphene in 2010 by Andre Geim and Konstantin Novoselov at the University of Manchester. With their unique structure, 2D materials has different and extreme properties compared to the other types of materials. Graphene, phosphorene, transition metal dichalcogenides and lately mxenes are the most popular types of two dimentional materials. These materials standout for energy storage applications by their extraordinary high electrical conductivity and high spesific surface area.

Graphene is a single layer of carbon atoms in two dimentional hexagonal lattice also known as honeycomb structure. Besides of its incredible mechanical properties, graphene also known as with its extraordianry electrical conductivity. Also, since it is just a layer of atoms, its spesific area is large which creates the perfect materials for supercapacitor applications.

Mxenes are transition metal carbides or nitrides that can be produced from etching the aluminum from MAX phase materials. These materials are layered structure with high surface area that makes it possible for ions to quickly intercalate between its layers and provides high surface area while conductive carbide layer provides quick charge transfer between ions and the transition metal.

2.4. Nickel Based Electrode Materials

Nickel oxides and hydroxide are popular electrode materials for energy storage devices with their high spesific area, high chemical stablity, low cost and environment friendly nature. As a member of metal oxide based electrode materials, their energy storage mechanism is mainly based on faradaic reactions.

2.4.1. Nickel oxides

Nickel is generally used in its oxide or hydroxide form as electrode material. Nickel oxides are highly popular due to their ease of production and high capacitances. They can be produced with various morphologies depending on the production method. Namely; chemical liquid precipitation, electrodeposition, sol-gel technique, molten salt synthesis and template method are the methods that can be used to produce nickel oxide. These methods are generally aims to produce different morphologies in order to produce nickel oxides with high spesific surface areas.

Even though nickel oxide electrodes possess high spesific capacitance for supercapacitor applications, their cycling stability and electrical conductivity is relatively low. Therefore, new studies focuses on adding new materials like polymers or carbon materials into nickel oxide electrodes in order to boost the capacity retention of these electrodes. In the meantime, carbon materials and conductive polymer additions can help to increase electrical conductivity. The reaction of nickel oxides when they are cycled in potassium hydroxide represented in the following equation:

$$NiO + OH^- \leftrightarrow NiOOH^- + e^-$$

2.4.2. Nickel hydroxides

Nickel hydroxides are the other popular member of the nickel based electrode materials. They are easily produced, environmentally friendly, cost efficient and thier capacitance is relatively high. These properties makes them popular for the energy storage applications. Nickel hydroxides have two different morphologies as alpha nickel hydroxide and beta nickel hydroxide.

Alpha nickel hydroxide is the first identified phase between two polymorphs. Its structure includes parallel oriented ß-$Ni(OH)_2$ layer to ab-plane that is intercalated by water molecules (Figure 2.8). The water molecules between layers can be detected by Raman and IR spectrum as O-H bonds [20]. Also, alpha nickel hydroxide possess a more disordered structure, (hydrotalcite-like) compared to the ß-$Ni(OH)_2$. Alpha nickel hydroxides have better electrochemical properties compared to the ß phase. However, the phase stability of alpha nickel hydroxide is relatively low. ß-$Ni(OH)_2$ is the more ordered polymorph of nickel

hydroxides as its isostructural with $Mg(OH)_2$ and ß phase is known with its higher electrical conductivity then alpha phase.

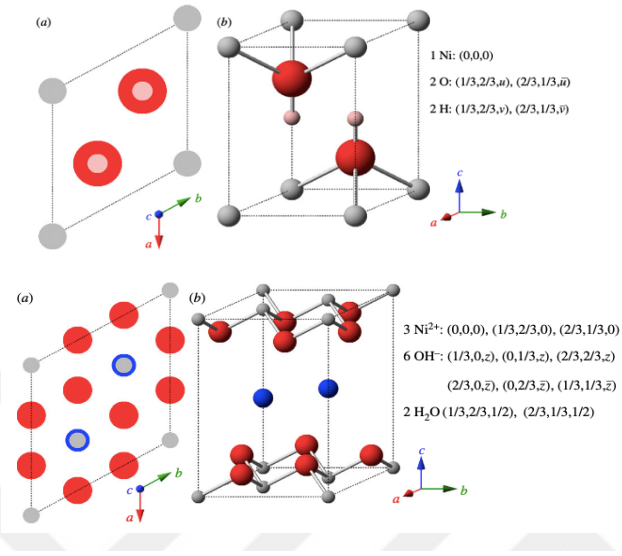

Figure 2.8. Crystal structure of A) ß- $Ni(OH)_2$ B) α-$Ni(OH)_2$.[20]

Nickel hydroxides follows the behaviour of transition metal oxide electrode materials for the energy storage mechanism as their main energy storage mechanism is faradaic reactions. Nickel hydroxides cycling is between its oxyhydroxide state and hydroxide state.

$$Ni(OH)_2 + OH^- \leftrightarrow NiOOH^- + H_2O + e^-$$

However, their stability in potassium hydroxide electrolyte is relatively low as alpha nickel hydroxide can transform to the beta nickel hydroxide by aging. In the meantime, as a result of aging, ostwald ripening occurs and particle sizes of the nickel hydroxide grows. Stress that occurs because of phase transformation causes the particle size growth. This greatly affects the energy storage performance of the nickel hydroxide as it decreases the electroactive surface area. Also, even though beta nickel hydroxides electrical conductivity is higher then alpha nickel hydroxide, electron transfer number is lower between β-$Ni(OH)_2$ - β-NiOOH redox couple then α-$Ni(OH)_2$ - γ-NiOOH .[21] When cycling, alpha nickel hydroxide cycles between gamma nickel hydroxide. However, after ageing, alpha phase transforms into beta phase and beta phase cycles between ß-NiOOH and itself. Therefore, until alpha phase completely

transforms into ß-$Ni(OH)_2$ cycling voltammetry would show 4 different peaks as two of them belongs to the alpha and gamma nickel hydroxide redox couple and two of them belongs to the beta nickel hydroxide and beta nickel oxyhydroxide.

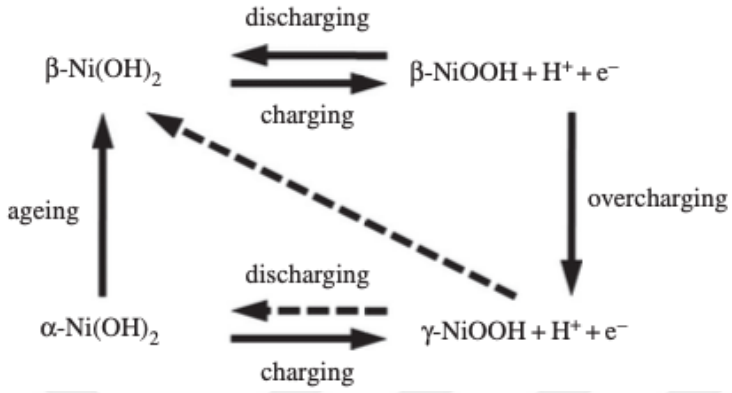

Figure 2.9. Charge-discharge cycles of $Ni(OH)_2$.[20]

Nickel based electroactive materials are popular for supercapacitor applications due to their high theorical capacitance, ease of production and environmentally friendly chemistry. The researches focuses on increasing the stability of the nickel based electroactive materials or producing new morphologies to enhance the spesific surface area therefore increase the performance. Kim et al. produced nickel hydroxides on 3-D dendritic nickel current collectors and obtained a high spesific capacitance 3637 Fg^{-1} at 1 Ag^{-1}. The increased surface area and direct contact between electroactive material and the current collector improved the performance. [22] Tokmak et al. used anodic oxidation technique in order to directly produce nickel oxyhydroxides on the nickel foam surface and obtained high capacitance 2.73 F/cm^2 at 1mA/cm^2. This method successfully produced flowerlike nickel oxyhydroxide on the nickel foam substrate which eliminates the binders that could effect the performance [23]. In the meantime, Zhang et al produced nickel hydroxide and polyaniline composite and high capacities (55 C/g at 0.5 mA/cm^2) and long cycle life (79% capacity retention at 2.5 mA/cm^2 after 2500 cycles) obtained. [24] Overall, nickel based elecctrodes are promising materials for supercapacitor applications and future work can focus on improving the stability while increasing the capacitance.

2.5. Mxenes

Mxenes are first synthesized by Yury Gogotsi and his research group in 2011. These materials are layered structure of metal carbides or nitrides that are produced by either selectively etching the “A” from the MAX phase materials or as thin films by using chemical vapor deposition or template method.

2.5.1. MAX phases

MAX phase materials are unique materials with combination of ceramic properties and metal properties. These materials have high electrical and thermal conductivity in the meantime, they are highly resistant to oxidation and thermal ceramics. With the general formula of $M_{n+1}AX_n$, “M” in the MAX symbolizes the transition metal while “A” symbolizes A-group element and “X” is either carbon or nitrogen (Figure2.10). MAX phases can be categorized by their stoichiometry; 211,312 and 413 phases represents the number of M layers located between each A-group element. More than 60 MAX phases are synthesized until know and majority of them 211 phases. [25]

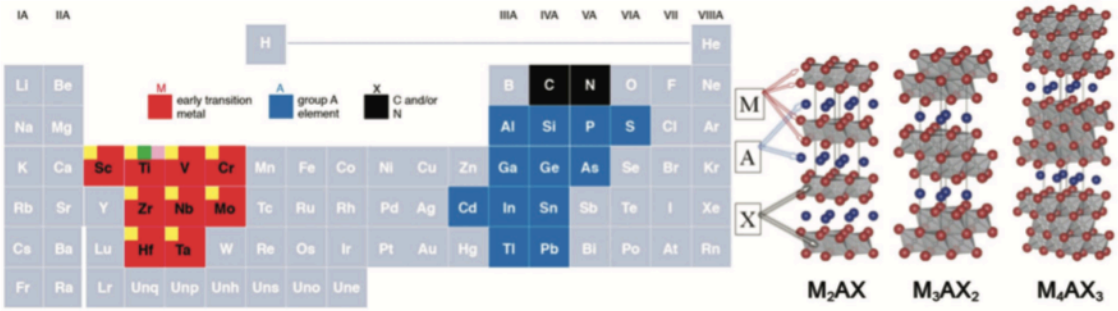

Figure 2.10. MAX strucutres and MAX phase elements positions in perodic table. [28]

2.5.2. Mxene structure

Mxenes are produced by the extraction of “A” from the MAX phases. As a result, structure of mxenes resembles MAX phases as M and X atoms locates in hexagonal lattice and X atoms are located at the center of edge-shared M octahedral cages. Therefore, instead of transforming to cubic strucure of MX, mxene layers can preserve the hexagonal structure with sixfold symmetry.

Mxenes also posesses typical flake features. Generally, height of one monolayer sheet of mxene is around 2.7 nanometers and interlayer distances around 1.5 nm [25]. Interlayer distance of mxene is higher than that of graphene and phosphorene and this is the reason of the general excitement about their usage in energy storage devices.

Terminations are the other aspects of the mxene structure. Since “A” layer is etched, remaining structure interacted with terminations such as oxygen, flourine or hydroxyl depending on the production method and environment [26]. These terminations can be determined by using XPS or other characterization methods such as RAMAN or FT-IR.

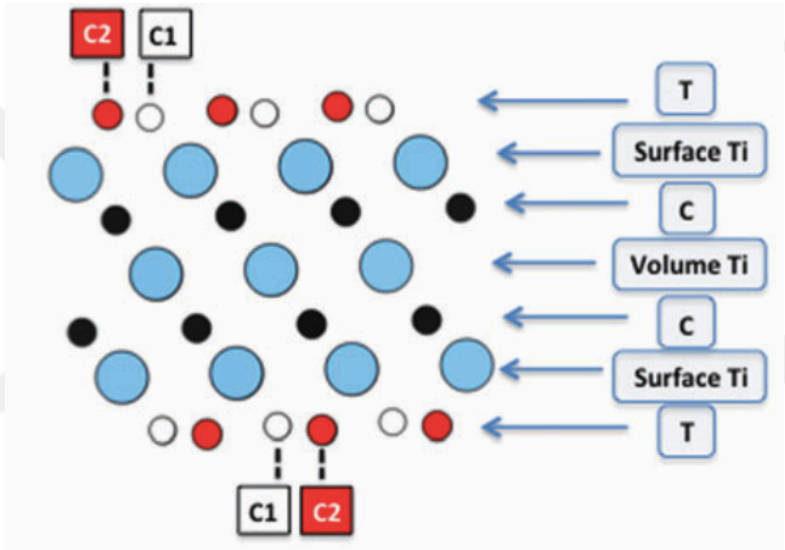

Figure 2.11. Mxene termination positions in structure. [26]

Termination surface groups play a huge role on the chemical and physical properties of mxenes. Specially, their effect on energy storage devices is immense as terminations have direct effect on capacity of the device. -OH and -O terminations are preferred over -F terminations due to higher capacitances, almost double of the mxenes with -F terminations [27]. The reason for this phenomenon is explained as intercalated water molecules display a favorable hydrogen bonding with -O and -OH terminations rather than -F terminations. [28] Therefore, studies focus on reducing -F terminations either in production process or with further surface modifications.

2.5.3. Mxene production

Mxenes can be produced from using variety of methods. Mainly, there are two approaches that can be named as bottom-up and top-down approaches.

2.5.3.1. Bottom up aproaches

Bottom up approaches includes chemical vapor deposition, template method and plasma enchanced laser deposition [29]. This approach has advantages like production of mxene without any floride terminations and produced mxenes are in high crystalline quality. Further, by using bottom up approach, stoichiometries like WC, TaC, TaN, MoN, that are not able to be produced with top bottom aproach can be produced. In CVD method, mxene is growth on the substrate that consists of Cu and Mo layers by heating the substrate above its melting point. Then, methane is introduced to the system and Mo_2C crystals are formated on the liquid Cu surface (Figure 2.12) [30], [31].

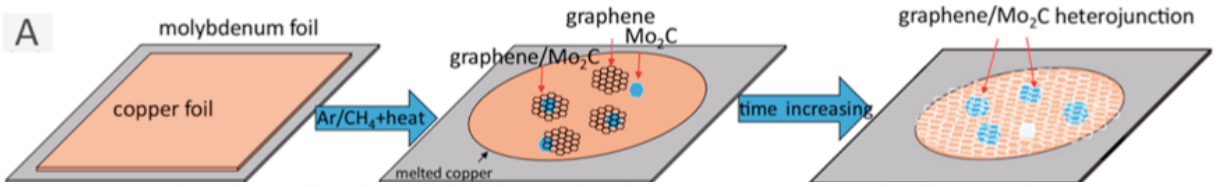

Figure 2.12. Production of mxenes by using chemical vapor deposition. [31]

Template method, compared to CVD, can produce with higher yield (Figure 2.13) . In that method, transition metal oxides are used as the templates and carbonization or nitridization occurs in order to produce transition metal carbides or transition metal nitrides.

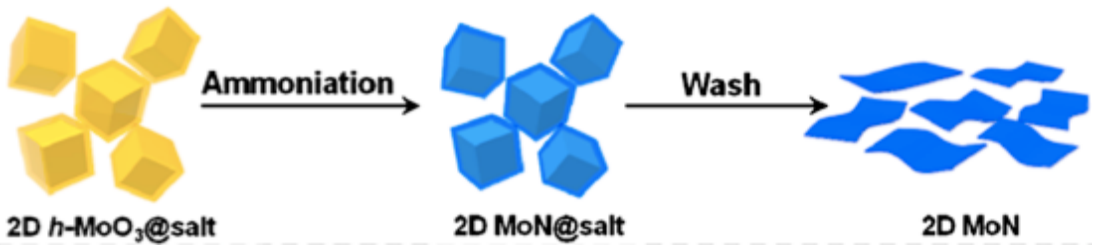

Figure 2.13. Mxene production by template method. [31]

In plasma enhaced laser deposition, process is similar to the CVD method. However, this process includes advantages of both CVD and pulsed layer deposition. CH_4 plasma is used to create high quailty Mo_2C films [32].

2.5.3.2. Top down approaches

Top down approaches includes creation of mxenes by etching "A" element from MAX phases. M-A bonds are metallic bonds meanwhile M-X bonds can show mixed behaviour of covalent/ionic/metallic. The bonds between M-A are too strong therefore it is hard to etch it mechanically.[33] However, high chemical reactivity of the A atoms makes it possible to chemically etching of these elements from the structure [28]. As a result of the etching, "A" layer is replaced by terminations which can be fluorine, oxygen or hydroxyl depending on the production method.

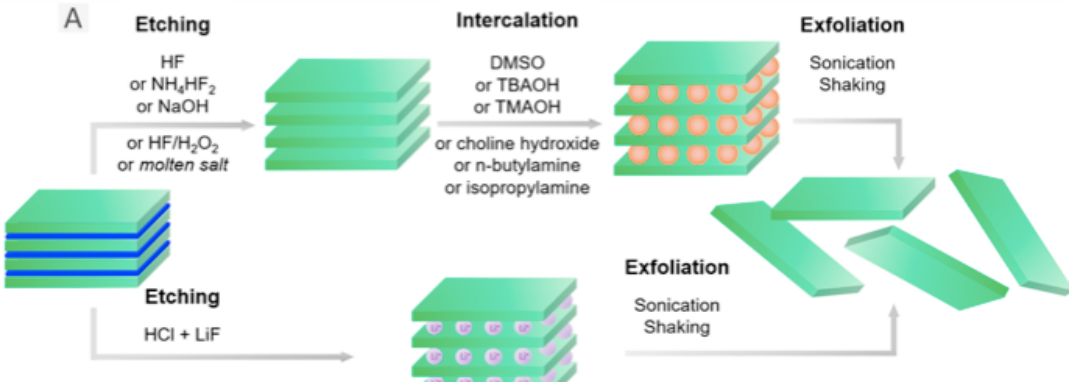

Figure 2.14. Bottom-up mxene production steps. [31]

Process follows the order of etching, intercalation and exfoliation. In the etching step, there are various etchants that are already used. Hydroflouric acid was the first etchant that has been used to etch "A" from the MAX phase. However, since it is a dangerous chemical and also it creates flourine terminations, studies were focused on new etchants. In situ HF method is one of these methods which uses 2 different etchants, HCl/ LiF and NH_4HF_2. When HCl/ LiF is used, lithium in the mixture behaves like an intercalant and therefore, there is no need for an extra intercalant. MAX powder is added to LiF/HCl and solution mixed for 24 hours. Resulting mixture is washed by using centrifuge until pH reaches to 5-6. Resulting mixture is vacuum filtered to produce

mxene powders. Compared to HF, the mxenes flakes that are produced with this method are larger which can be advantegous for energy storage applications. In addition, the mxenes that are produced by HF method has four times more -F terminations compared to the mxenes that are produced with LiF/HCl method.[34] In the meantime by using same etchant, mxene clay can be produced with MILD method. This method uses the same etchant with different LiF/HCl ratios and resulting mxene is in the clay form. Further, it can be produced as mxene paper which can posess superior peformance for energy storage applications.

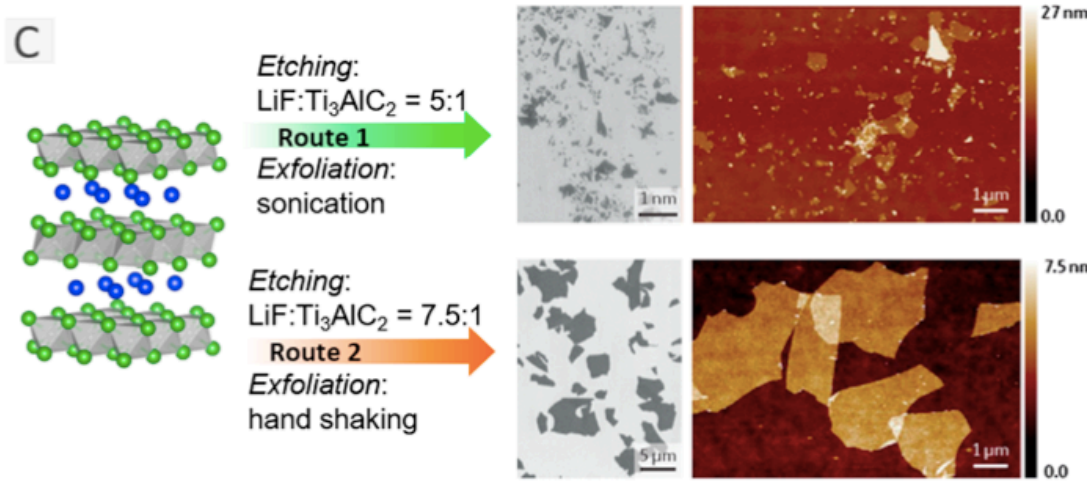

Figure 2.15. Mxene flake sizes according to production methods. [31]

There are also other methods discovered in order to remove flourine usage from the etching process in order to reduce flourine termination. HCl and NH_4Cl/TMAOH are two electrolytes that are used to etch "A" from MAX phase electrochemically. By using these electrochemical methods, mxenes can be produced without flourine terminations however production yield is limited. When etching step is completed, process continues with intercalation and exfolation. In the intercalation step, an organic solvent is used to intercalate between layers. These intercalants can be DMSO, TBAOH, TMAOH etc. In the exfolation step, sonication or shaking is applied to exfoliate the layers by using already intercalated organic solutions. Resulting colloidal suspensions should be stablized with adaquate solvents in order to prevent aggration and oxidation.

Produced mxenes are generally in powder form and therefore, they should be coated on surfaces in order to be used on energy storage devices. Coating methods are prefered depending on the application. For example, spin coating method prefered for the optics and electronics due to its ability to produce uniform coatings. Vacuum filtration method is one of the methods prefered for the energy storage device application. In this method, mxene colloidal solution is obtained on membrane filter by using vacuum. Depending on the production method, produced mxenes can be used as selfstanding mxene papers.

Figure 2.16. Coating methods of mxene powders onto substrates. [33]

Electrophoretic deposition is one of the effective methods for producing mxene coatings for the energy storage applications due it is ability to produce high quality binder-free film electrodes. In this method, electrical field is applied between electrodes and the charged particles in the collaidal suspension coated on the surface on the electrode depending on the zeta potentials of the particles. This method can be applied with aqueous or non-aqueous electrolytes. However, in aqueous electrolytes potential that can be applied is limited due to bubble formation caused by water electrolysis can affect the coating quality. Therefore, non-aqueous electrolytes such as acetone can be preferred over water. Compared with other coating methods, electrophoretic deposition have advantages like production of uniform coatings and variety of the possible coatings. The coating thickness or mass load can easily be adjusted by coating time. Also,

electrophoretic coating method found to be reducing the agglomeration of mxene and helps to retain the conductivity and improve the accesibilty of the electrolyte to the electrodes.[35]

2.5.4. Stability of Mxenes

Oxidation and restacking of mxenes are one of the issues of mxenes for the applications. Both in production and storage, oxidation of mxenes are one of the challanges that should be considered. Titanium in the mxene structure can quickly get oxidized into TiO_2 in time scale between hours to days. Oxidation starts from the edges and then proceeds with nucleation and eventually grows through whole surface [36]. As a result of oxidation, the black collodial solution turns into gray colloidal solution because of the color of TiO_2. In order to prevent the oxidation, storage conditions are crucial. Fastest oxidation is occured when mxenes are stored in water (4 days) with the exposure to the oxygen and slowest oxidation is obtiained with iso-propanol solvent and argon environment (4752 days). It is also stated that solvent is much more effective then the environment in these cases as iso-propanol solvent and O_2 environment can oxidize mxene in 2026 days while water solvent argon environment can oxidize mxenes in 41 days [37].

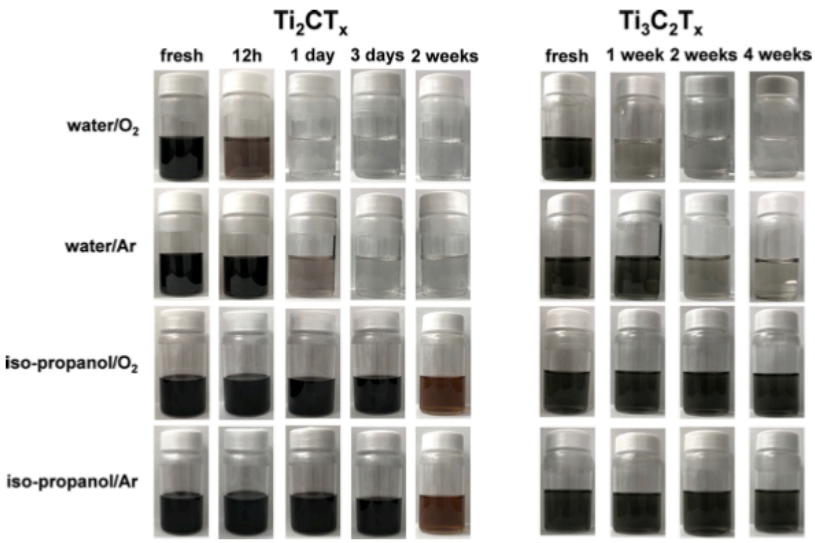

Figure 2.17. Oxidation of mxenes in different kinds of atmosphere and media. [37]

However, in other researches, temperature of the storage, UV exposure and storage media are stated as other important parameters. Solid media that can be obtained by freeze drying of mxene powders, considered as a better storage condition for the mxenes and liquid media gave

worse results as conductivity of mxenes decreased more than 65% after 1 week of storage in water. Decrease in conductivity is related with the increase in TiO_2 content in the material. Additionally, study shows that in order to extend the lifetime of mxenes before oxidation, UV exposure should be limited. The mxene powders that are exposed to UV loses over 85% of its conductivity in 24 hours while the powders that are kept in the darkness loses the same conductivity percentage in 27 days[38]. Therefore, a refirigated, oxygen-free, dark environment is adviced for storage of mxenes in order to avoid oxidation. In addition, in inert atmospheres, mxenes are stable up to 840ºC. Above that temperature, mxenes begin to transform their cubic structure like TiC in Ti_3C_2 case [39].

2.5.5. Mxene in energy storage applications

Energy storage devices are one of the popular applications for mxenes. Surfaces and interfaces plays a huge role on the performance of energy storage devices as they greatly effect ion intercalation, adsorption and chemcial reactions. Therefore, two dimentional materials are in huge demand in these aplications due to their unique structure. Specially, mxenes has several advantages over other two dimentional materials; first of all, its metallic electrical conductance can provide electrons to all electroactive sites, secondly, transition metals in its structure can introduce faradaic reactions with its redox reactions, third, the two dimentional nature and water molecules that are intercalated in the synthesis process can improve ionic transportation, and finally, conductive layer of carbon can rapidly transfer the charges (Figure 2.18) [40].

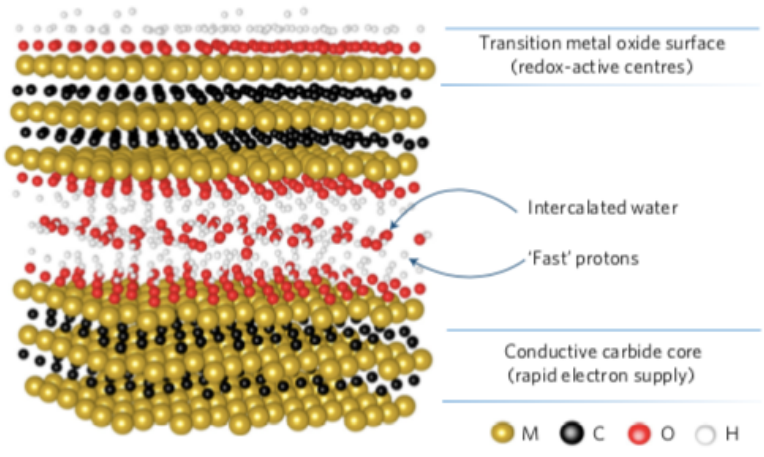

Figure 2.18. Charge storage mechanism of mxenes. [40]

Mxenes can be used in various energy storage devices such as batteries and supercapacitors. Due to its unique layered structure, various ions such as Li, Na, K, Mg, Ca can intercalate between layers. Thus, making other metal-ion batteries possible other than Li-ion batteries.

2.5.5.1 Battery applications for mxenes

The variety of possible chemical and structural prospects of the mxenes makes them a great candidate for battery applications. The main mechanism of mxenes charge storage during charge and discharge is continious change in the oxidation state of the transition metal.Based on the therotical calculations M_2C mxenes performs better in batteries than other vareities of mxenes since 2 layers of M host one layer of Li in M_2C and 3 layers of M host one layer of Li in M_3C_2 mxenes. In the meantime, according to same study, O terminations are performing better in these applications because it provides extra Li layers to be absorbed on the lithiated mxenes[41]. Furthermore, besides the terminations, transition metal in the mxene structure also as crucial for the performance. Studies show that V_2CT_x mxene provides the highest Li ion capacity compared to the other mxenes. In addition, Nb_2CT_x shows higher gravimetric capacity ($180mAhg^{-1}$) over Ti_2CT_x 110 ($mAhg^{-1}$) at the same cycling rate.[42]. Mxenes can be used as anodes in Li-ion batteries where graphite anodes cannot met the reqiured capacities. According to theorotical calculations, mxenes are suitable for the Li-ion anodes as they have a low operating voltage and their lithium storage capacity is high.[43]

Mxenes can also be used with another material to create a composite electrode to avoid interlayer distance decrease due to restacking resulting with a lower electrical conductivity and electroactive surface area. Therefore, additional materials such as carbon nanotubes are combined with mxenes. Study shows that carbon nanotube addition to the mxene can increase the capacity of the battery to 320 $mAhg^{-1}$ which is almost twice of the bare mxene. Carbon nanotubes in the structure helps to distribution of ions and also forming a 3d conductive network thus decreasing the contact resistancebetween mxene particles.[44]Moreover, mxenes can be used with other metals to form a composite. For example, SnO_2 decorated Ti_3C_2 mxenes are produed with hydrothermal method to increase the performance of mxene electrodes and an ultrahigh capacity of 1030 $mAhg^{-1}$ at 100 mAg^{-1} is obtained. However, the stability of this electrode was quite low as it drops to 360 $mAhg^{-1}$ after 200 cycles which can be a result of the hydrothermal method since mxenes can get quickly oxidized in that environment.[45] Another study changed the production method to a low temperature atomic layer deposition and

SnO_2/Ti_3C_2 electrode coated with HfO_2 in order to enhace the stability of these electrodes. As a result, electrode was able to keep its spesific capacity at 843 $mAhg^{-1}$ after 50 cycles at 500 mAg^{-1}.[46]

In the meantime, mxenes are used in other metal-ion devices since they can provide the ability of hosting these metal ions with their high interlayer distances. Na-ion intercalation mechanism on mxene sheets are investigated and increase of interlayer disance from 9.7 to 12.5 A is observed. This is attributed to first Na^+ intercalates and acts as a pillar to keep the interlayer distance sufficient sodiation/desodiation. [47] Carbon nanotube/Ti_3C_2 composite showed improved ion accesbility and enhaced volumetric capacity of 345 $mAhg^{-1}$ at 100mAg^{-1} after 500 cycles. [48] Meanwhile, titanium carbonitride is prepared for potasium-ion batteries and achieved 710 $mAhg^{-1}$ at 20 mA/g however its capacity dropped to 275 $mAhg^{-1}$ after first cycle.[49]

2.5.5.2. Supercapacitor applications for mxenes

Mxenes are popular for the supercapacitor applications due to their high interlayer distance that makes it possible to host various ions and provide access to electroactive areas. Ti_3C_2 is the most widely studied mxenes among all. The first reports for the high capacitance mxenes was Ti_3C_2 paper electrode with 350 Fcm^{-3} which is much higher than the carbon based electrode materials.[50] Following this, 900 Fcm^{-3} reported [51] by the production of the mxene clay electrodes that would already be comparable of the capacitances of highest obtained capacitances for metal oxide electrodes. And finally, mxene hydrogels are produced and the volumetric capacitance is reached to 1500 Fcm^{-3} that reaches to unmatched RuO_2 supercapacitor electrode capacitance[40]. Therefore, mxenes can be classified as a high potential material for the supercapacitors.

Energy storage mechanism of mxene in supercapacitor applications is still being investigated. The cycling voltammogram graph of mxene resembles the double layer capacitors since there are no distinct peaks that would symbolize faradaic reactions observed. In alkali electrolytes, there is an electric double layer formation that provides the charge storage by the hydrated cations in the interlayer space [52] . However, when an acidic electrolyte like H_2SO_4 is used, the CV curve of mxene looks like a distorted rectangular shape. A detailed investigation found out that the mechanism of mxenes in sulfuric acid is mostly pseudocapacitive since change in the oxidation state of the Ti is observed[53].

In another research [54], a comparison between H_2SO_4 , $(NH_4)_2SO_4$ and $MgSO_4$ has been made in order to have a better understanding of the energy storage mechanism. While H_2SO_4 is used, hydronium in H_2SO_4 bonds with the O termination in the $Ti_3C_2T_x$ negative electrode upon discharging and debonds while charging. This bonding and debonding changes the valance state of the Ti thus resulting a pseudocapacitive performance. However, in $(NH_4)_2SO_4$ and $MgSO_4$ electrolytes, only electric double layer mechanism is observed. In the meantime, charge storage routes found to differ as it is ion exhange in H_2SO_4 where as it is counterion adsorption in $(NH_4)_2SO_4$ and $MgSO_4$ electrolytes (Figure 2.19). However, there are still ongoing researches about the energy storage mechanism of the mxenes. The main difficulty of these researches is mxenes properties and performance are strongly influenced by its production method. Especially, transforming the flourine terminations into oxides with chemical modifications increased the enhanced the capacitance by a factor of two to seven. [55]

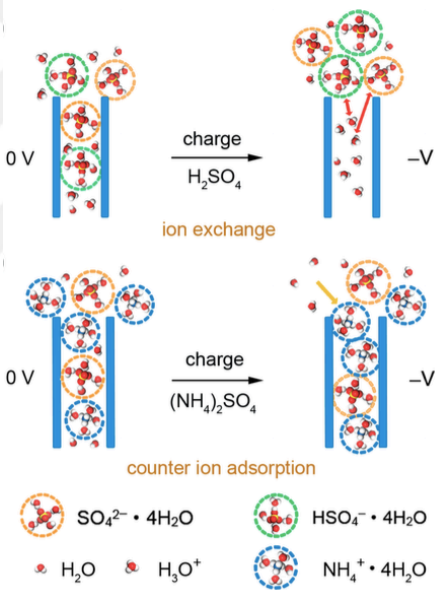

Figure 2.19. Charge storage of mxenes in H_2SO_4 and $(NH_4)_2SO_4$.[54]

Mxenes are also used with different kinds of electrode materials in order to enhance a better performance by creating a composite material. TiO_2/Ti_2CT_x nanocomposite that has been produced by the surface oxidation of the mxene. TiO_2 in the structure increases the interlayer distance as well as the surface area however the performance of these electrodes were not enough as it was 51 Fg^{-1} [56]. In the meantime, nickel oxides are grown on mxene by using a

hydrothermal method and the capacity is increased from 8.2 $mAhg^{-1}$ to 60.7 $mAhg^{-1}$ when it is compared to bare mxene electrode. This is attributed to enhanced electrolyte ion diffusion into the electrode. [57] Also, mxene and nickel alumium layered double hydroxide composite is produced by using mxene as a substrate and superior spesific capacitance of 1061 Fg^{-1} at 1 Ag^{-1} and retained 70% of its capacitance after 4000 cycles. [5] Meanwhile, poylmers can be also used to create a composite with mxenes. Polymers that includes polar functional groups are able to intercalate between $Ti_3C_2T_x$ mxene layers and prevent restacking of mxene layers and improve the mechanical properties of the mxene paper [58]. Overall, mxenes with their high surface area and layered strucutre that enhances the diffusion properties are forefront for supercapacitor applications.

3. EXPERIMENTAL PROCEDURE

In experimental procedures used in this thesis work is described under four headings:- 1. synthesis of max phase, 2-Synthesis of mxene (conversion of max to mxene) 3. Synthesis of NiOOH and 4. Electrophoretic deposition process for production of mxene films and composites

3.1. Synthesis of MAX Phase

Ti_3AlC_2 MAX phases produced by molten salt synthesis by using from Ti powder, aluminum powder and carbon black powder in the molar ratio of 3:1.1:1.8 with the addition of NaCl and KCl 50%:50%. The mixture was mixed 10 hours by using agate balls and ethanol in an agate jar. Resulting slurry dried at 60ºC for 10 hours in air. The mixture is then heated in a tube furnace by a heating speed of 4ºC/min to 1250 ºC and held for 3 hours followed by cooling at the same ratio of 4ºC/min. Obtained Ti_3AlC_2 MAX phases washed and dried to clean it from salts.

3.2. Synthesis of $Ti_3C_2T_x$ Mxene

LiF+HCl method has been used for production of $Ti_3C_2T_x$ mxene. This method has been selected because this method does not directly involves HF, there is no additional intercalant need since Li^+ ions behaves like intercalants and mxenes produced by this method includes less flourine terminations. Parameters are optimized with different molarity of etchant as well as different reaction temperatures. 1.6 g LiF is added to 20ml of 9M HCl and stirred for few minutes. 0.5g of Ti_3AlC_2 is added to the etchant and left for 24h with continuous stirring at 45ºC. The resulting acidic mixture is washed with deionized water by using centrifuge. 5 min per cycle at 3500 rpm is selected as centrifuge parameters. The washing cycles are repeated until pH reaches to 4-5. Once pH reaches to 4-5, resulting mixture left for centrifuge for 1h. Produced supernatant is separated and remained slurry mixed with water and centrifuged for 1

hour again. Resulting supernatant and sediment is vacuum filtered by using polymer membrane and mxene powders are collected on the filter.

3.3. Synthesis of NiOOH

NiOOH is produced by using anodic oxidation technique. Parameters of this production method has been concluded by a former study of our laboratory group [23]. Before starting to procedure, nickel foams are cleaned by ultrasonicated in %10 HCl for 10 min followed . Nickel foams then collected and connected as anodes for anodic oxidation technique while graphite crucible is connected as cathode. Anodic oxidation took place in KOH electrolyte at 200ºC for 30 minutes. Potential applied between electrodes is set to 0.8V.

3.4. Electrophoretic coating of mxenes

Mxenes are coated on NiOOH by using electrophoretic deposition. 50 ml of acetone (Merck %99) and 0.003 g of I_2 mixed then mxene powder is added. 2 nickel foils are used as the anodes on the both sides of cathode and NiOOH produced nickel foam is used as cathode. 50V is applied between electrodes and coating time is set at 5 minutes.

3.5. Characterizations

All electrochemical characterizations conducted in 6M KOH electrolyte by using Ag/AgCl as referance electrode and platinum mesh counter electrode. Biologic SP-150 potentiostat/galvanostat system has been used for all electrochemical measurements. Electrochemical impedance measurements has been studied at room temperature at open circuit potential using a signal of 5mV amplitude in the frequency range of 100 kHz to 0.1 Hz.

Morphological investiagtions has been conducted with field emission secondary electon microscope (FE-SEM) (JEOL JSM7000F). Structural investigations has been conducted by using micro-RAMAN (LabRam 800, Horiba Scientific, Jobin Yvon, France) and X-ray Diffractometer (PANalytical X’pert PRO).

4. RESULTS AND DISCUSSION

4.1. Optimization of Parameters of Production Methods

4.1.1. Mxene production

MAX phase produced by molten salt synthesis which effectively worked. Figure 4.1 represents the XRD of the MAX powders obtained. The peak at 9.5 º (002) diffraction peak represents the d spacing of 9.27 Aº which is comparable with the literature [59].

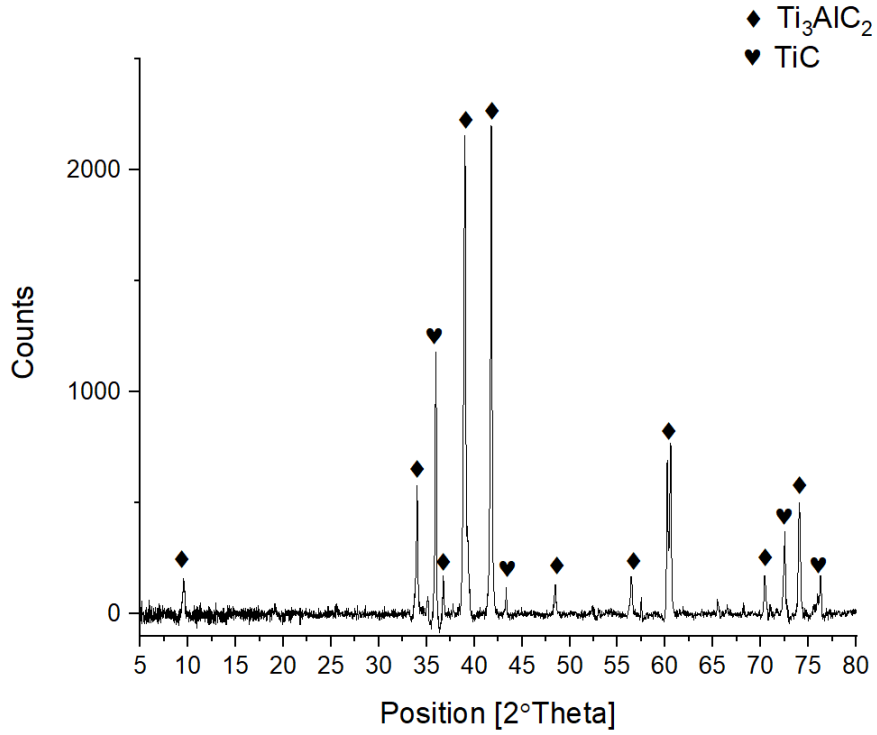

Figure 4.1. XRD pattern of synthesized MAX phase.

Mxene powders are produced by using LiF+HCl production method. Firstly, LiF+HCl method is used with 7.5M LiF+9M HCl and experiment is conducted at room temperature.

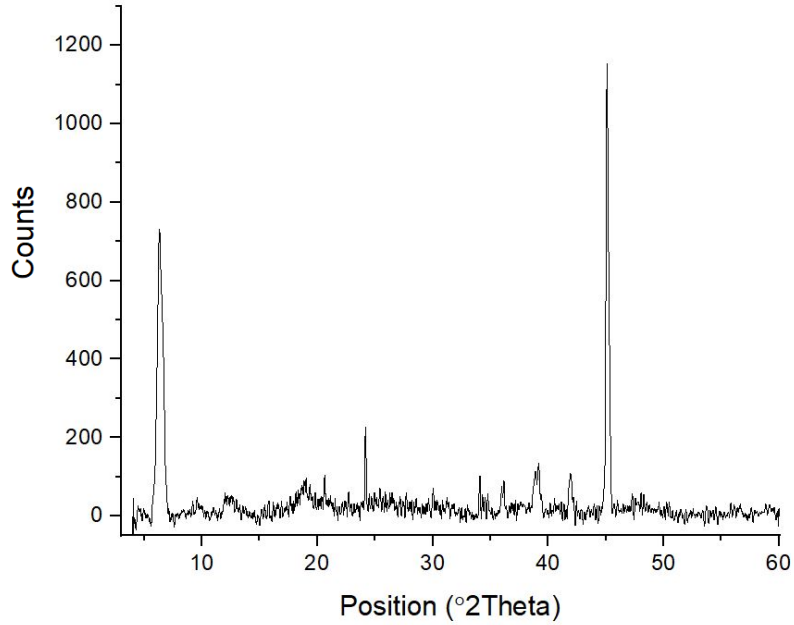

Figure 4.2.XRD pattern of mxenes produced by 7.5 M LiF/9M HCl etchant in RT.

Figure 4.2 shows the XRD of the resulting powder from the 7.5M LiF+9M HCl experiment. Even though the peak at 9.5 º shifted towards the lower angles that symbolizes the etching of the “A” from the MAX phase, there are still intense MAX phase peaks observed on the figure.

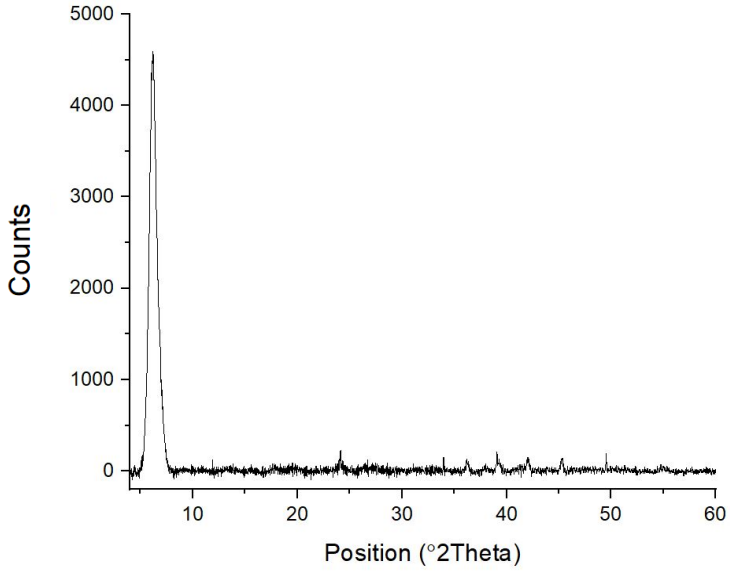

Figure 4.3. XRD pattern of mxenes produced by 12 M LiF/9M HCl etchant in RT.

The results were not satisfying enough. Therefore, 7.5M LiF/9M HCl method is changed to 12M LiF/9M HCl (MILD method [33]) in order to obtain higher yield of etching.

Figure 4.3 represents the XRD results of the mxene powders that are produced with 12M LiF/9M HCl. The increase in the peak at 6.5 º compared to Figure 21 is observed. MAX phase peaks were decreased substantially. However, the peaks did not completely disappear.

Further, the temperature of the experiment increased to 45ºC. According to reports [60], increasing the temperature to 45-50ºC improves the etching yield.

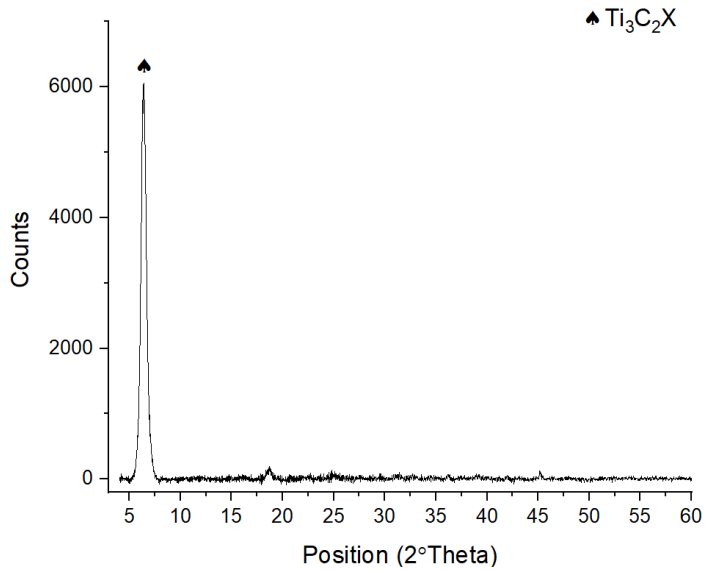

Figure 4.4. XRD pattern of the mxene powders that are etched in 12M LiF/9M HCl at 45ºC.

Figure 4.4 represents the XRD results of the mxene powders that are obtained by using 12M LiF/9MHCl at 45 ºC. The MAX peaks almost completely dissapeared and a high yield of mxene powders are obtained. The (002) peak which is located at 9.5 º for MAX phase shifted towards to 6.27º which represents 14.8 Aº d spacing. This parameters are verified as optimum parameters in order to obtain high quality mxene and used for the further experiments.

4.1.2. Electrophoretic deposition

Electrophoretic coating has been conducted according to the procedure given in the literature [35]. First, 0.5 g I_2 50 mL acetone and 0.1g mxene powder is used as the electrolyte. However,

the bubble formation effected the surface of the electrode. Flowerlike nickel oxyhydroxide structure flaked off (Figure 4.5) and due to high amount of bubbles, mxenes cannot be coated.

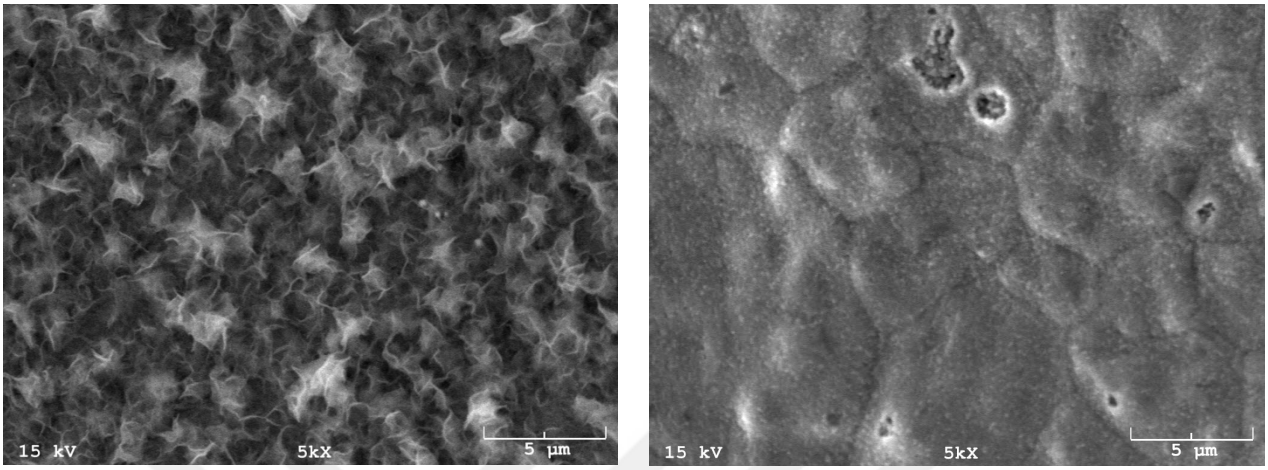

Figure 4.5. SEM images of NiOOH electrode before and after electrophoretic deposition in electrolyte that consist 0.5g I_2.

The iodine amount is decresed on next experiment in order to prevent bubble formation. According to literature [61], 0.1g per liter is suggested. Therefore, the amount of iodine is decreased to 0.003g. No bubble formation is observed during experiment and mxenes could be succesfully coated on the substrate (Figure 4.6)

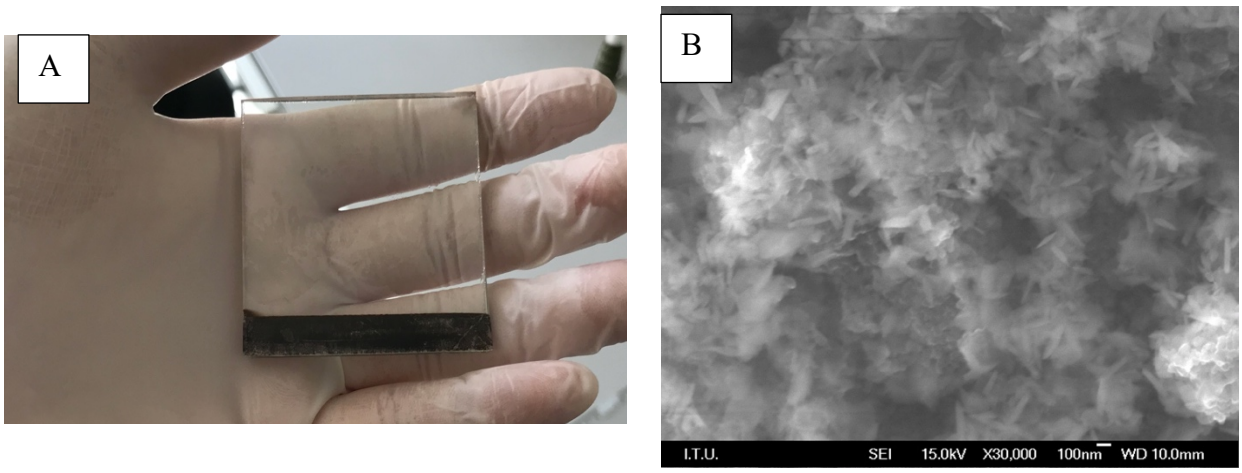

Figure 4.6. A) Mxene coatings on FTO glass that are produced in electrolyte that consists 0.003g I_2 B) Mxene flakes coated on nickel foam with electrolyte that consists 0.003g I_2.

4.2. NiOOH Sample

NH electrodes are characterized and tested to obtain a reference in order to see the mxene coating effects on performance of nickel oxyhydroxide electrodes. Structural, morphological and electrochemical aspects of the electrodes are investigated.

SEM and RAMAN has been conducted before and after cycling for 1000 cycles in order to see the morphological and structural changes on NiOOH electrodes. Due to highly defective structure of nickel hydroxides, XRD is not preferred for characterizations and micro -RAMAN is used for structural analysis.

Figure 4.7 represents the SEM images of produced NiOOH samples. Flowerlike structure of the NiOOH has been observed.

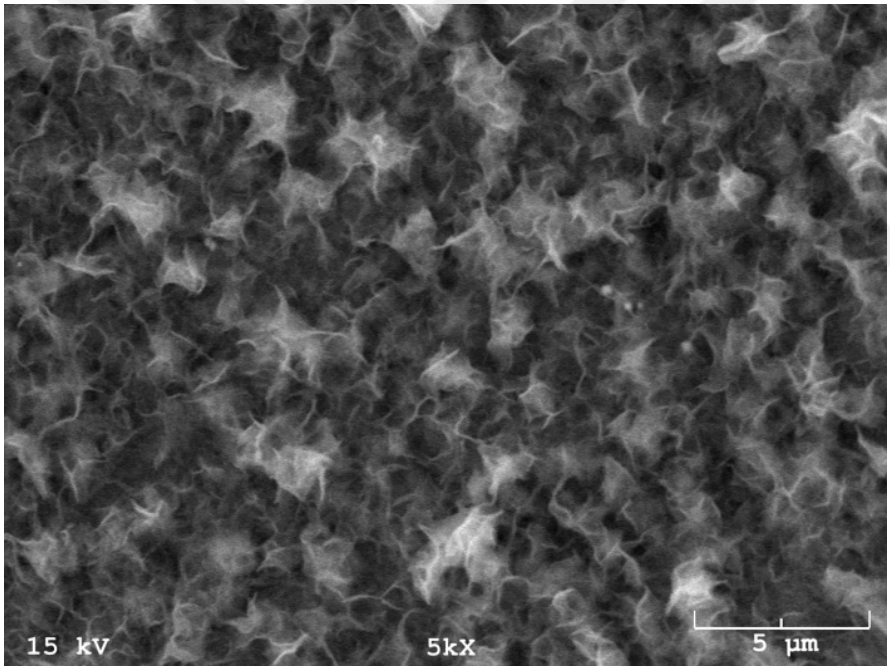

Figure 4.7. SEM image of NH electrode.

Figure 4.8 represents the RAMAN spectrum of the NH electrode before cycling. The bands at 479 cm^{-1} and 556 cm^{-1} corresponds to the Ni-O vibrations in NiOOH. However, both γ-NiOOH and β-NiOOH display two bands at these same wavenumbers. In order to differenciate between

these two phases, the ratio of the intensity of peaks at 479 cm^{-1} and 556 cm^{-1} should be considered. When the intensity peak at 479 cm^{-1} is higher than 556 cm^{-1}, γ-NiOOH is obtained and if the intensity of the peak at 556 cm^{-1} is higher, β-NiOOH is obtained.[62] Therefore, any phase transformation from γ-NiOOH to β-NiOOH can be detected by using RAMAN.

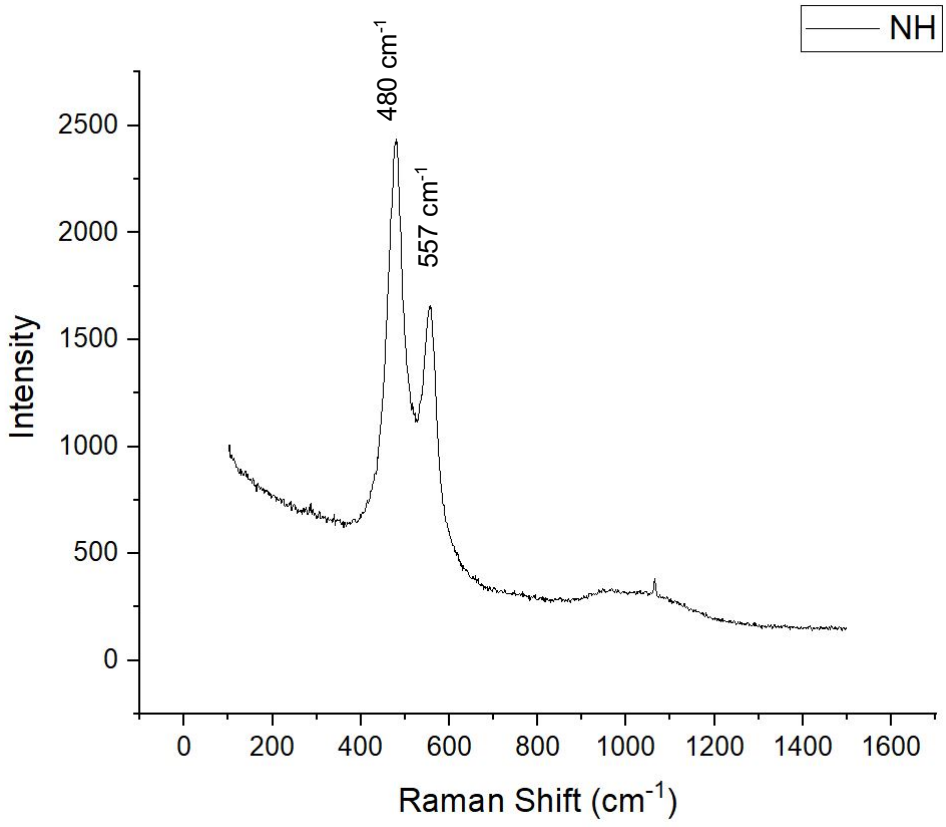

Figure 4.8 Raman spectrum of NH sample before cycling.

Figure 4.9 represents the cycling voltammogram of NiOOH samples that are cycled with 20 mv/s scan rate. The electrode is cycled for 1000 cycles in order to observe the performance of NiOOH. In the first cycles, peaks at 420 mV at anodic side and 120 mV at cathodic side corresponded to 66,5 mA/cm^2 and -76 mA/cm^2 current densities respectively. However, peaks started to shift towards each other during cycling with decreasing current densities which can be a sign of phase transformations of the NiOOH. Capacitance of the electrode is calculated according to Equation (2).

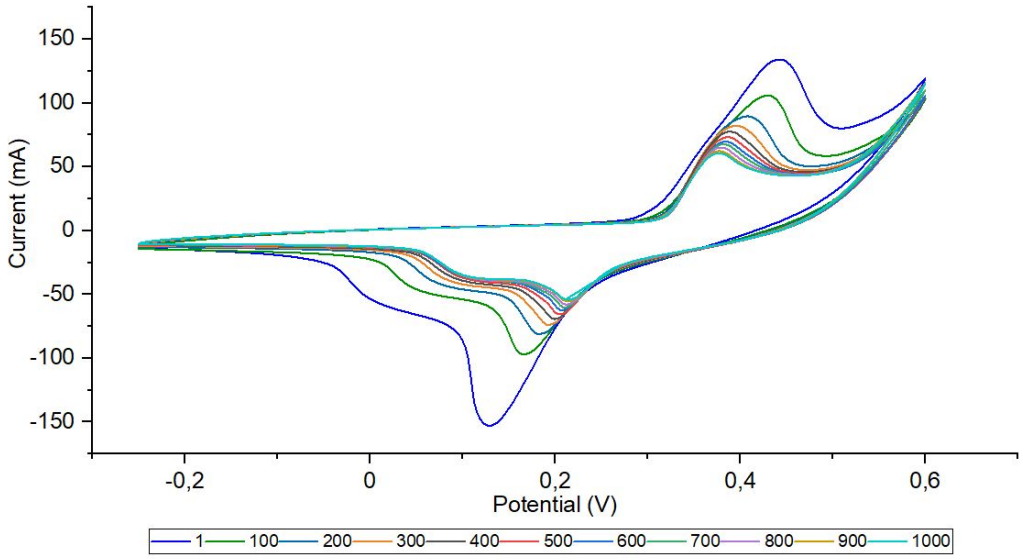

Figure 4.9. Cycling voltammogram of NH sample in 6M KOH vs Ag/AgCl reference electrode.

Capacitance of the electrode was 1.15 Fcm^{-2} at the first cycles and it decreased to 0.539 Fcm^{-2} after 1000 cycles which corresponds to 46% capacity retention. Moreover, freshly prepared

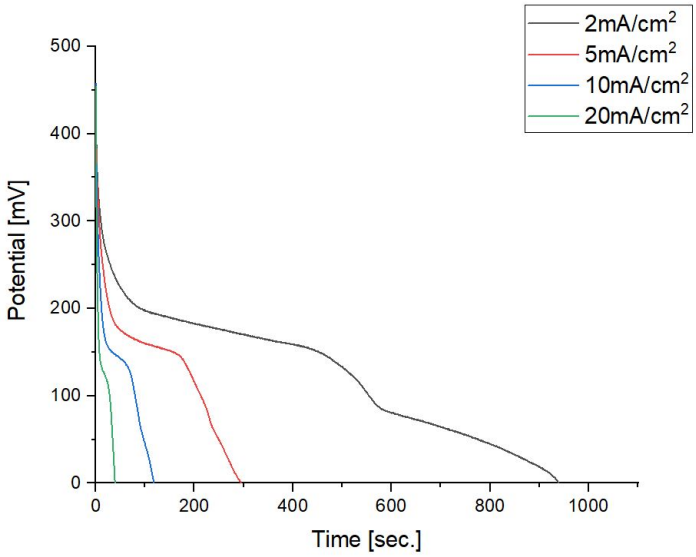

Figure 4.10. Discharge curves of NH sample various current densities

samples werw also subjected to galvanostatic charge-discharge tests. Tests were conducted by using various discharge currents in order to evaluate discharge current dependent behavior and performance of the NH electrode.(Figure 4.10). Capacitance of the electrode from galvanostatic charge discharge test has been calculated by Equation (3). Highest capacitance is obtained at 2mA/cm^2 as 4.24 F/cm^2 while the lowest capacitance is obtained at 20mA/cm^2 as 1.72 F/cm^2.

Furthermore, scan rate dependent cycling voltammogram curves are obtained in order to evaulate the pseudocapacitive behavior of the electrode (Figure 4.11). Equation 4 is used for the characterization of the electrode in energy storage mechanism aspect.

$$i = a \times v^b \tag{4}$$

i = Current (mA)

v=scan rate

a,b=constants

According to Equation (4) the constant b represents the behavior of the electrode. “b” can be calculated as the slope of the logi vs logv graph. When b is equal to 0.5, reaction mechanism is completely diffusion controlled and when b is equal to 1 reaction mechanism is surface controlled [63]. Following this, b constant of the NH electrode is calculated as 0.547 which

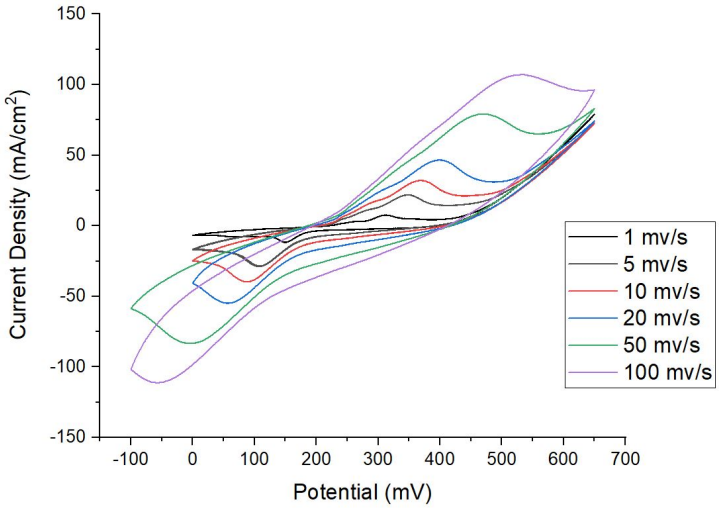

Figure 4.11. Cyclic voltammogram of NH sample at different scan rates.

means reaction is controlled by both diffusion and surface mechanism however highly diffusion controlled.

Moreover, EIS has been conducted to get more information about electrochemical properties of NH electrode (Figure 4.12) R_s+C1/(R_{ct}+W2+Q1)+Q2/R3 is used as the equivalent circuit for both before and after cycling of the sample. This cirucit has been used for the similar composite electrodes that are prepared in this study (graphene and $Ni(OH)_2$) [64]. Nyquist plot shows a small semi circle in the high frequency region and a linear Warburg part in the low frequency region which shows the capacitive behaviour of the sample. R_s values before cycling was 0.642 Ω and it decreased to 0.584 after cycling. This result was expected as beta nickel hydroxides resistance is lower than other phases of nickel hydroxides [65]. The R_{ct} before cycling was 0.019 Ω and it increased to 2.397 Ω after cycling which explains the dramatic drop of the capacitance of the electrode.

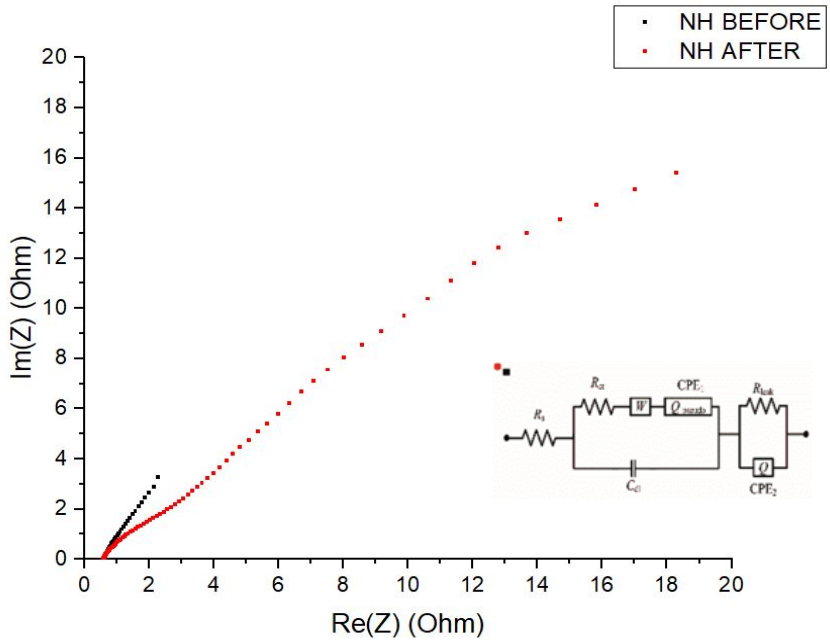

Figure 4.12. Nyquist plot of the NH sample.

In order to confirm the phase transformation that could be observed in cycling voltammogram and EIS, RAMAN is conducted to cycled samples (Figure 4.13). Moreover, the intensity of the

peak at 559 cm^{-1} surpassed the peak at 479 cm^{-1} which confirms the phase transformation to β phase.

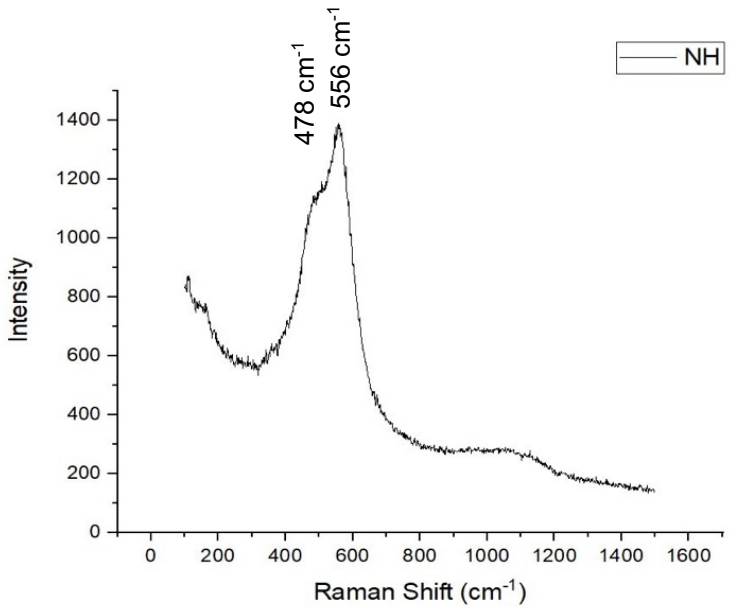

Figure 4.13. Raman spectra of NH sample.

Meanwhile, SEM images are taken from the cycled samples in order to check the effects of cycling. Figure 4.14 represents the SEM images of NH electrodes after 1000 cycles. There are no significant changes observed in the flowerlike morphology of the NiOOH.

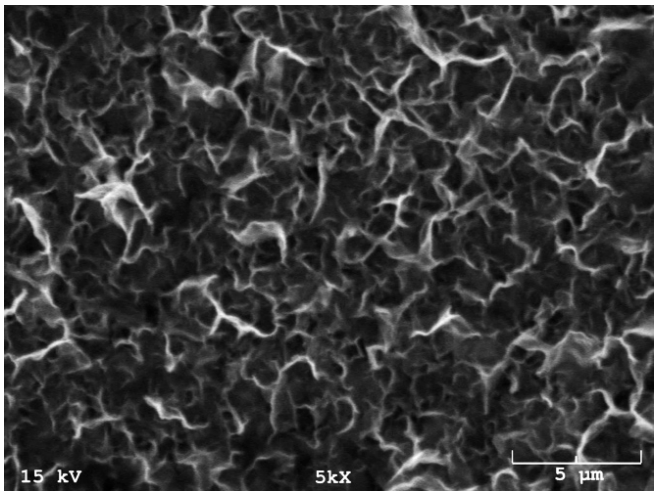

Figure 4.14. SEM image of NH after 1000 cycles.

4.3. Mxene Electrode

Mxene electrode has been tested with the same procedure as NH electrode in order to obtain a second reference and conclude the benefits of the composite electrode. Structural, morphological and electrochemical aspects of the electrode are investigated. SEM and RAMAN investigations has been conducted before and after cycling for 1000 cycles in order to see the morphological and structural changes on mxene electrodes.

Figure 4.15 shows the mxene flakes that are coated on the nickel foam with electrophoretic deposition. The length of mxene flakes were in the range of 400 nm to 1.7 microns.

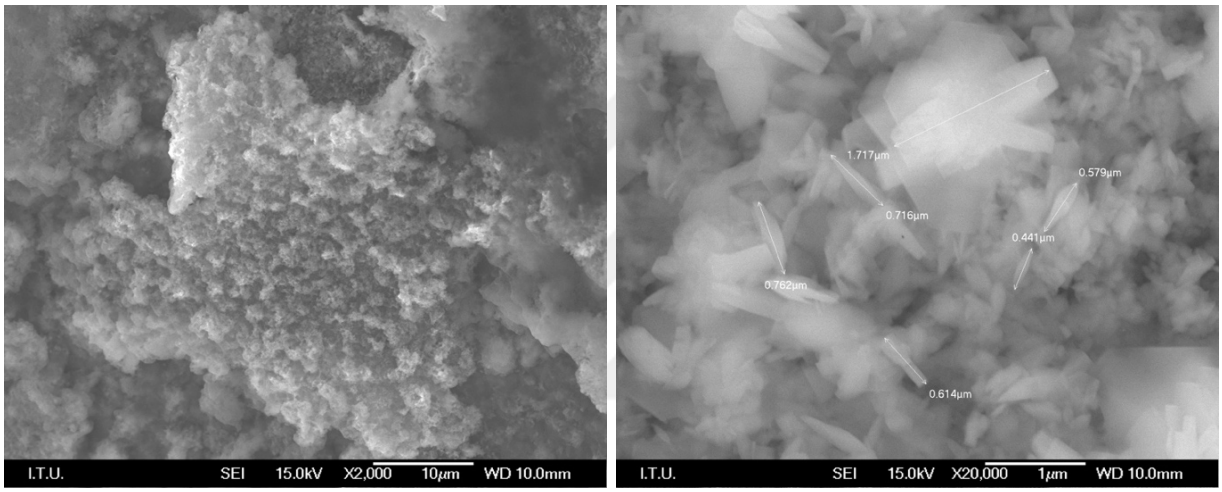

Figure 4.15. SEM images of mxene electrode before cycling.

Mxene electrode inspected with RAMAN in order to investigate the structure of the mxenes and detect possible oxidation after cycling (Figure 4.16) . D band around 1380 cm^{-1} corresponds to the disordered carbons while G band around 1590 cm^{-1} corresponds to the sp^2 carbon bonds in the structure. Increasing intesnity of the D peak means increasing amount of disordered carbons which is the sign of oxidation of mxenes [66]. Increase of the disordered carbons are attributed to migration of titanium atoms bonding with oxygen, leaving carbon sheets alone [36].

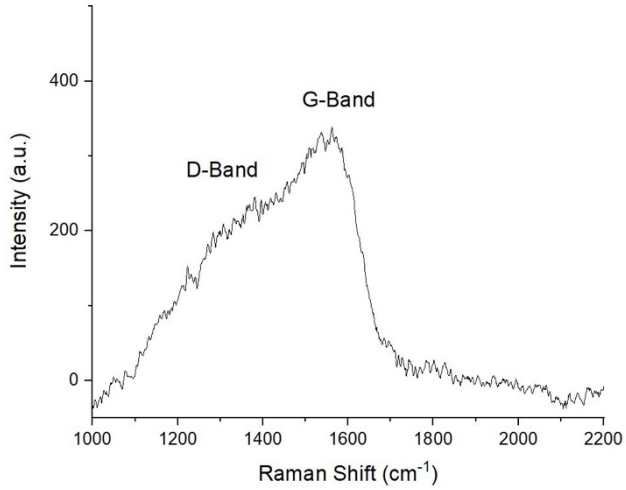

Figure 4.16. Raman spectra of mxene electrode before cycling.

Cycling voltammetry has been conducted on the mxene electrode in order to obtain information about mxene electrodes electrochemical performance. The parameters of the cycling is the same with the NH electrode however potential window of the mxene electrode determined to be narrower when compared to the NH electrode.

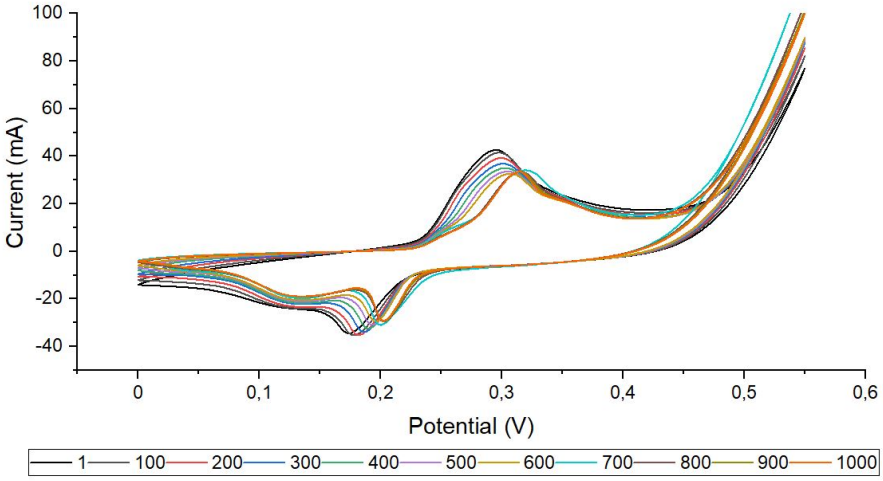

Figure 4.17. Cyclic voltammogram of mxene electrode in 6M KOH vs Ag/AgCl.

Figure 4.17 represents the cycling voltammogram of the mxene electrode. At the initial cycles peak at 177 mV in the cathodic side and peak at 297mV at anodic side has been observed. However, these peaks are shifted during cycling which is a sign of structural change. In the meantime, currents are decreased in addition the to peak shifts. Capacitance of the mxene electrode has been calculated by using Equation (2), as 0.41 F/cm^2 at the first cycles and the capacitance is reduced to 0.298 F/cm^2 after 1000 cycles which corresponds to 72% capacity retention.

Moreover, galvostatic charge-discharge tests has been conducted on various discharge currents in order to evaluate discharge current dependent behavior and performance of the mxene electrode.(Figure 4.18). Capacitance of the electrode from galvostatic charge discharge test has been calculated by Equation (3). Capacitances are calculated for each current densitiy and similar capacitances obtained 0.34 F/cm^2 , 0.29 F/cm^2, 0.26 F/cm^2 and 0.22 F/cm^2 for the current densities of 2mA/cm^2, 5 mA/cm^2,10 mA/cm^2 and 20 mA/cm^2 respectively.

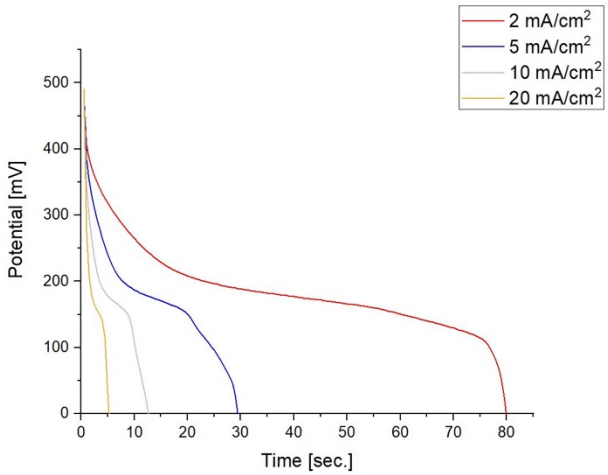

Figure 4.18. Discharge curves of mxene electrode at different discharge current densities.

Cycling voltammetry test has been conducted on different scan rates in order to observe the scan rate dependent current densities and obtain information about reaction mechanism of mxenes(Figure 4.19) . From Equation 4, the b value is obtained as 0.541 which means reaction is controlled by both diffusion and surface. Pseudocapacitive behaviour of the mxenes can be attributed to oxygen terminations in the structure[67].

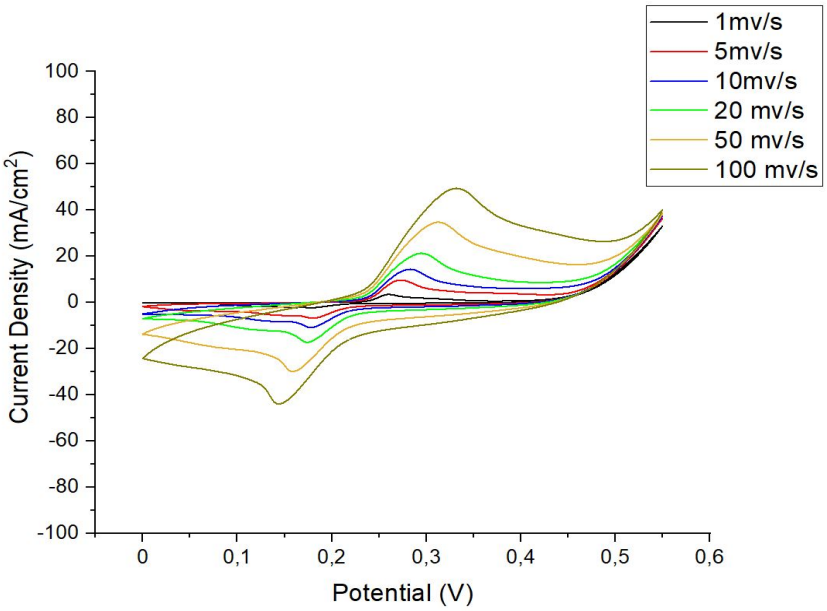

Figure 4.19 Cycling voltammogram of mxene electrode at different potential scan rates.

Figure 4.20 represents the raman spectra of mxene electrode. D band at 1380 cm^{-1} is increased and broadened which means disordered graphitic carbon in the structure is increased. Therefore, oxidation of mxenes are confirmed with Raman spectroscopy.

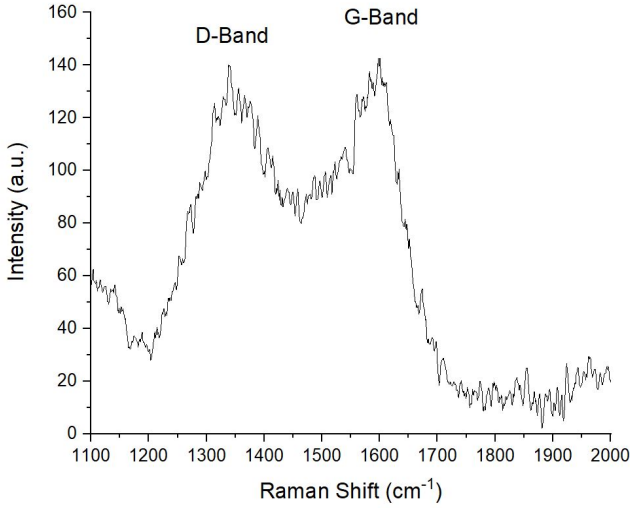

Figure 4.20. Raman spectra of mxene sample after 1000 cycles.

Furthermore, electrochemical impedance spectroscopy has been used to obtain more information about mxene electrodes eletrochemical performance. Figure 4.21 represents the nyquist plot obtained from the EIS of mxene electrode. Rs of the mxene before cycling was 0.474 Ω and it increased to 0.478 Ω after 1000 cycles. Rct values are calculated as 0.031 Ω before cycling and it increased to 0.149 Ω after 1000 cycles

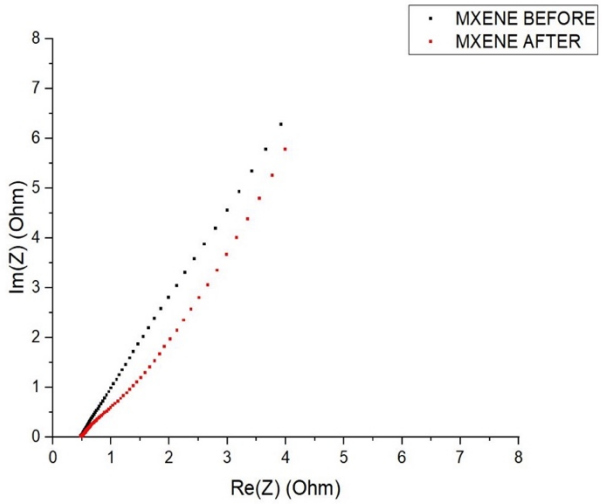

Figure 4.21. Nyquist plot of mxene electrode.

Moreover, Figure 4.22 represents the SEM images of mxene electrode after 1000 cycles. The flaky morphology of the mxenes dissapeared and it turn into a more compact structure. This can be a result of the oxidation of mxene and therefore phase transformation.

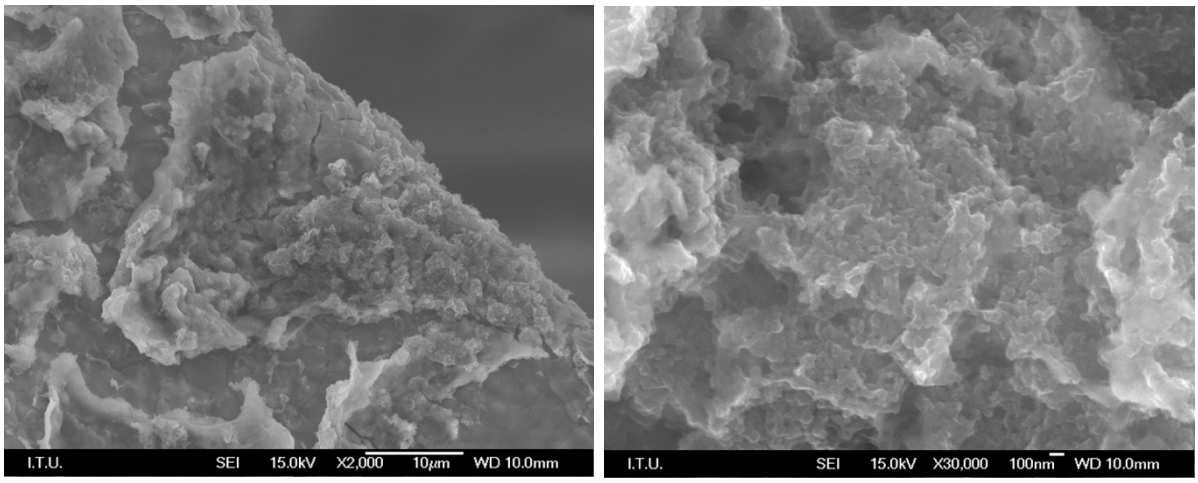

Figure 4.22. SEM images of mxene electrodes after 1000 cycles.

4.4. NiOOH/Mxene Composite Electrode

The same characterization steps that has been conducted for NH and mxene electrode also conducted for the nickel hydroxide/mxene electrode.

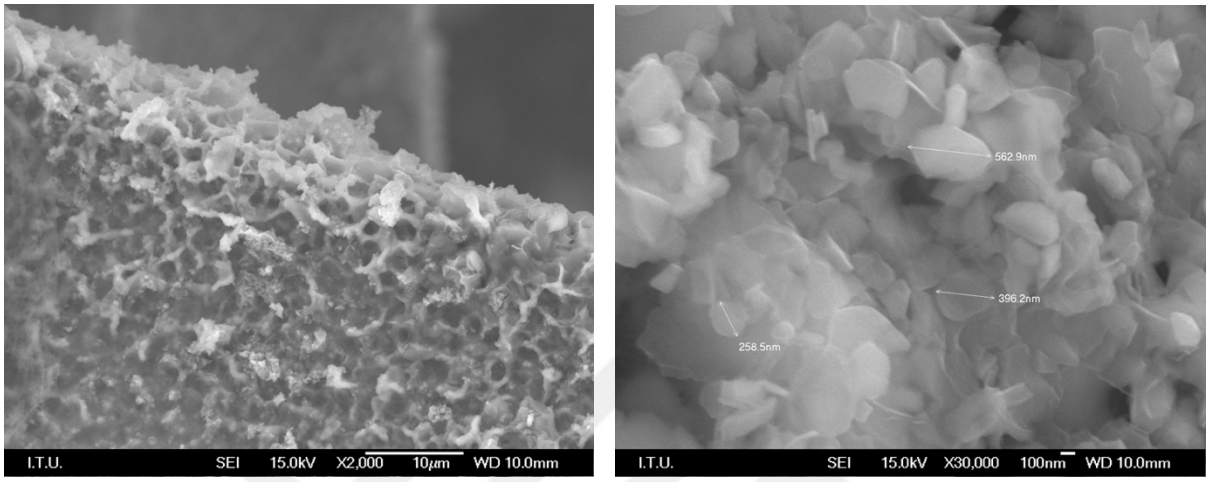

Figure 4.23. SEM images of NHM electrode before cycling.

Figure 4.23 represents the SEM images of NHM electrode before cycling. It has been observed that mxene flakes are coated on the flowerlike structure of the nickel oxyhydroxide. Flake sizes differ from 258 nanometers to 562 nanometers.

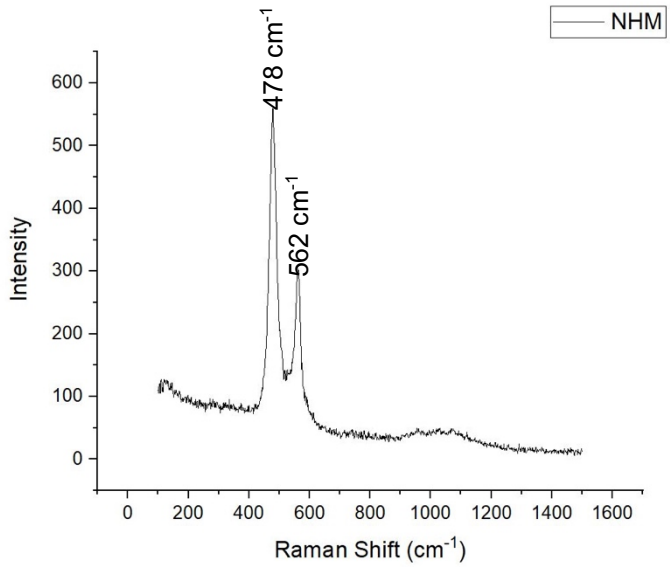

Figure 4.24 Raman spectra of NHM electrode before cycling.

Figure 4.24 represents the RAMAN analysis results of NHM sample. Same peaks are observed as NH electrode which corresponds to γ-NiOOH structure. This result also confirms that electrophoretic deposition method does not effect the structure of NH. Following this, electrochemical performance tests has been conducted.

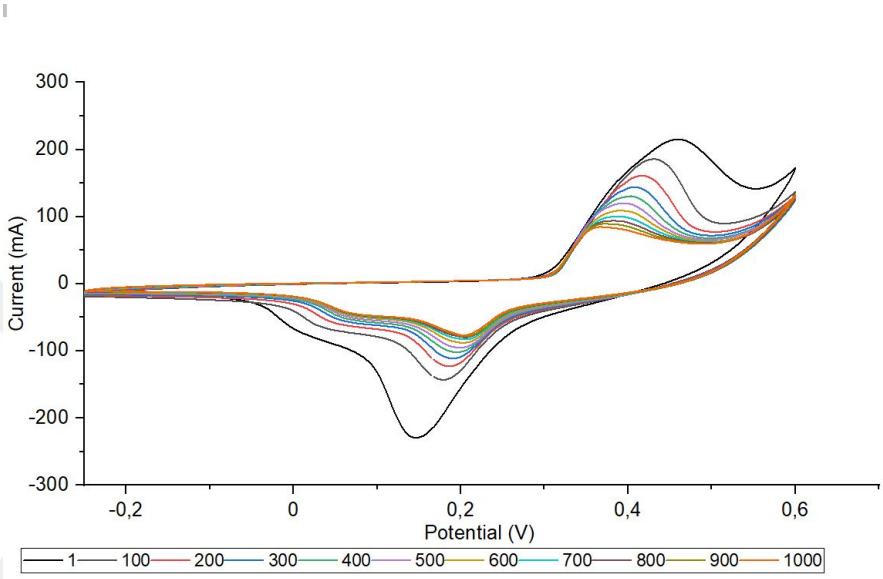

Figure 4.25. Cycling voltammogram of NHM electrode in 6M KOH vs Ag/AgCl.

Cycling voltammetry has been conducted in order to obtain information about electrochemical performance of the NHM electrode (Figure 4.25) There are no additional peaks observed other than NiOOH cycling peaks. Meanwhile, the same behaviour of cycling observed. The peaks started to shift towards each other while cycling which is a sign of a phase transformation. The current densities at the peak positions were 115 mA/cm^2 and -114 mA/cm^2 at the first cycles and it dropped to 42.1 mA/cm^2 and 38.3 mA/cm^2 after 1000 cycles. The areal capacitance of the NHM electrode was 1.9 F/cm^2 at the first cycles then it dropped to 0.814 F/cm^2 after 1000 cycles which corresponds to 42% capacity retention. Galvostatic charge-discharge tests has been conducted on various discharge currents in order to evaluate discharge current dependent behavior and performance of the NHM electrode (Figure 4.26).

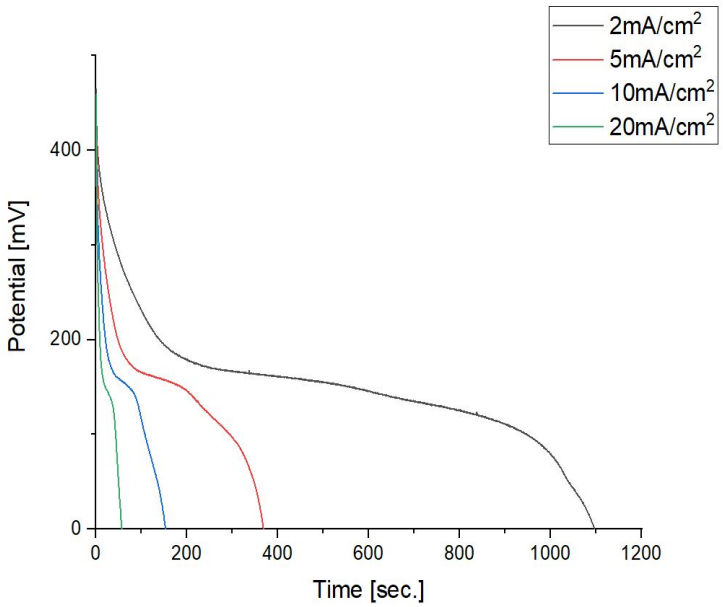

Figure 4.26. Discharge curves of NHM electrode at various discharge current densities.

The capacitances also calculated according to Equation (3). Areal capacitances of 4.72 F/cm^2 , 4.02 F/cm^2, 3.82 F/cm^2 and 2.48 F/cm^2 are calculated for current densities of 2 mA/cm^2 , 5mA/cm^2, 10 mA/cm^2 and 20 mA/cm^2 respectively.

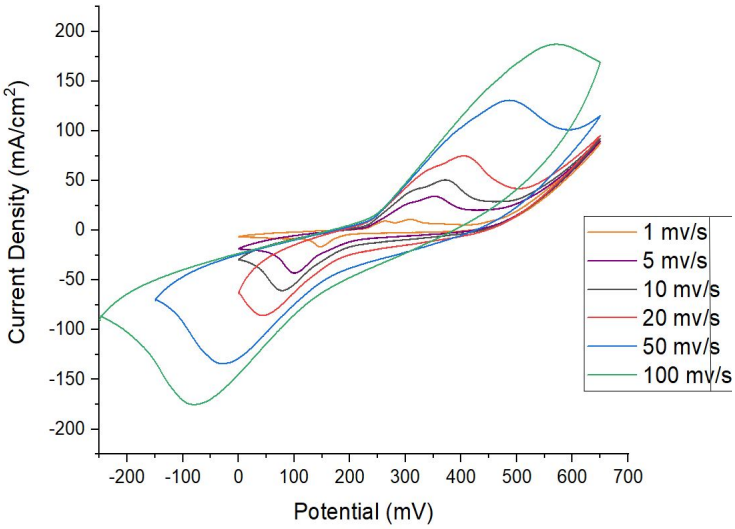

Figure 4.27. Cyclic voltammogram of NHM electrode at different scan rates.

Meanwhile, scan rate dependent cycling voltammogram curves are obtained in order to evaulate the reaction mechanism of the electrode (Figure 4.27). Equation (4) is used for the characterization of the electrode in energy storage mechanism aspect. “b” value is calculated as 0.573 which means reaction is controlled by both diffusion and surface reactions.

Figure 4.28 represents the nyquist plot of the NHM sample before and after 1000 cycles. After cycling, the slope of the veritcal line in the nyquist plot is decreased which is a sign of reduced charge transfer properties. Equivalent circuit fitting has been conducted with the same circuit that has been used for NH sample. Furthermore, R_s of the NHM sample before cycling was 0.329 Ω and it increased slightly to 0.372 Ω after cycling. R_{ct} of the NHM sample was 0.019 Ω before cycling and it increased to 1.752 Ω after cycling.

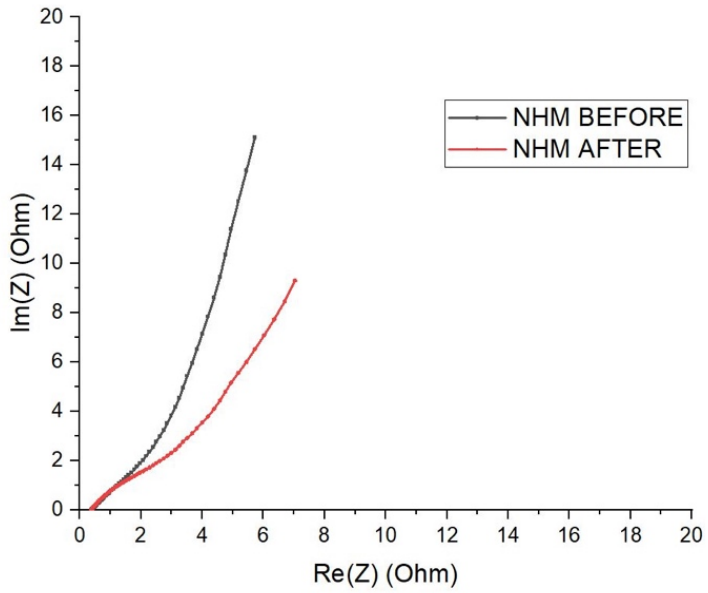

Figure 4.28. Nyquist plot of NHM electrode.

Figure 4.29 represents the RAMAN spectra of the NHM sample after 1000 cycles. Similarly to NH sample, phase transformation to ß-NiOOH is occurred as the peak at 556 cm^{-1} surpassed the the peak at 479 cm^{-1}.

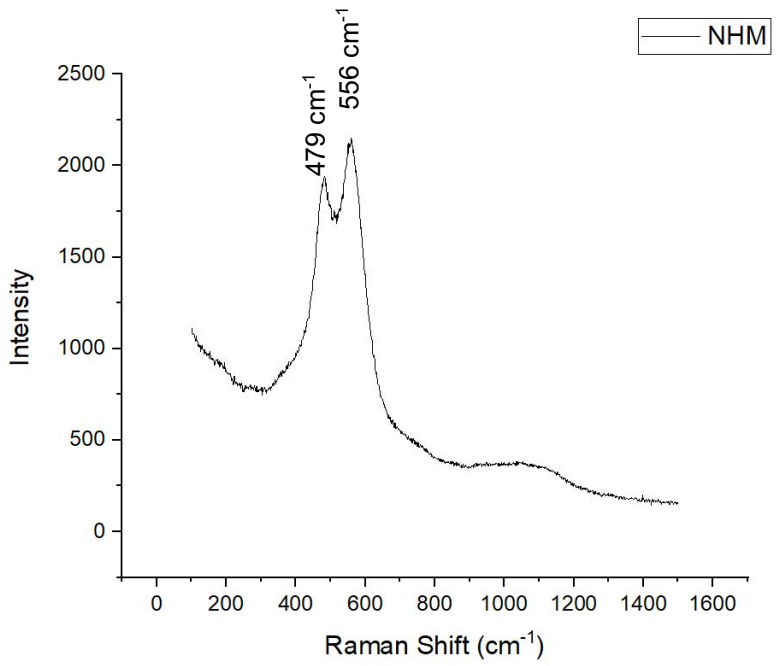

Figure 4.29. Raman spectra of the NHM electrode after 1000 cycles.

Finally, morphological investigations has been conducted by using SEM (Figure 4.30). Morphological behaviours of mxene and NH electrodes are also reflected into their composite. While flowerlike structure remained stable, flaky structure of mxene dissapeared and more compact morphology of mxenes are obtained.

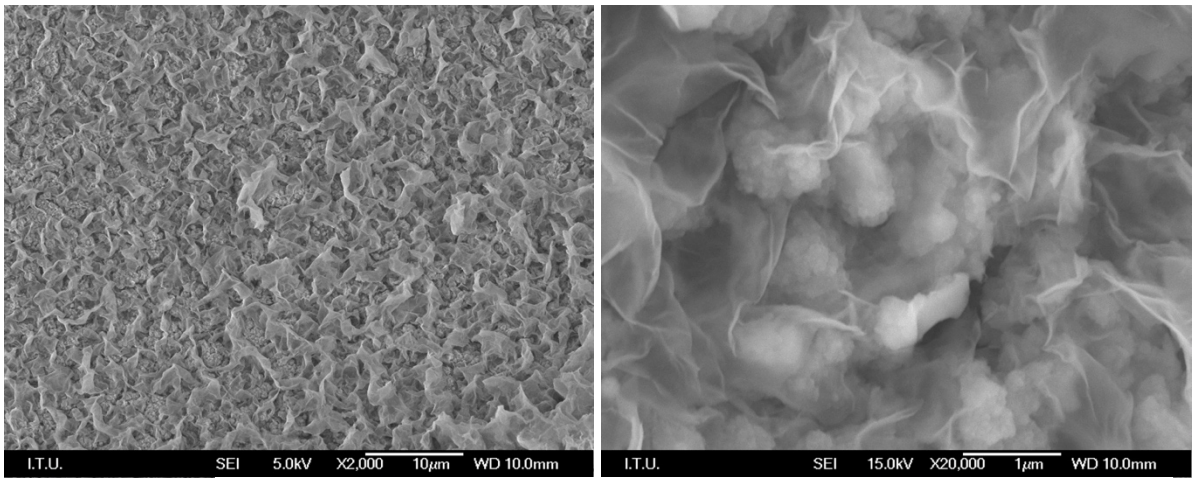

Figure 4.30. SEM images of NHM electrode after 1000 cycles.

5. DISCUSSION

Nickel oxyhydroxide, mxene and composite mxene/nickel oxyhydroxide electrodes are prepared and characterized in order to understand the contribution of mxene coatings to the nickel oxyhydroxide electrodes. First of all, when electrochemical performances are compared, it has been observed that composite electrode exhibited a higher capacitance (1.91 F/cm^2) compared to nickel oxyhydroxide (1,15 F/cm^2) electrodes at a scan rate of 20mv/s. (Figure 5.1A)When mxene electrode is characterized, it posses 0.41 F/cm^2 at the scan rate of 20 mv/s therefore increase of the capacitance cannot be explained by simply addition of their capacitances and working separately. Meanwhile, mxene coating did not seem to be helpful for the capacity retention of the NHM electrode (Figure 5.1B) almost the same with NH electrode (42% for the NHM electrode 46% for the NH electrode) .This can be attributed the degradation of the mxene in the structure resulting in slightly less capacity retention of NHM electrode. After all, even though mxene coatings greatly improve the spesific capacitance of the electrode, it is not helpful for the cycling stability.

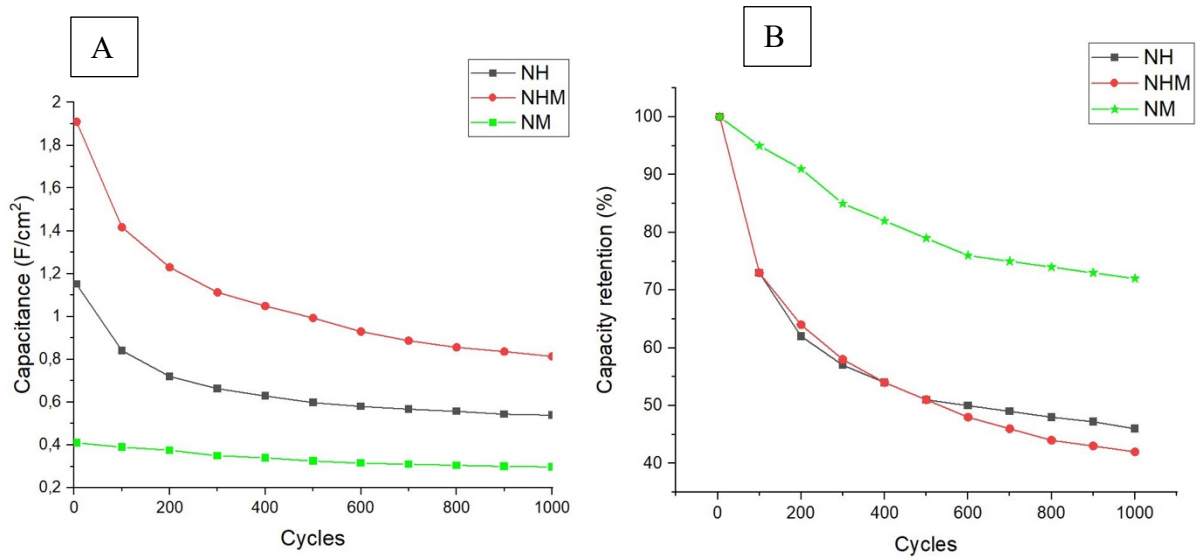

Figure 5.1. A) Cycle dependent areal capacitances B) Cycle dependent capacity retention.

When RAMAN spectra are compared before and after cycling of NH and after cycling of NHM electrode, the phase transformation of gamma nickel oxyhydroxide to beta oxynickel hydroxide is still observed (Figure 5.2). Therefore, cycling stability of the NHM is similar to the NH electrode.

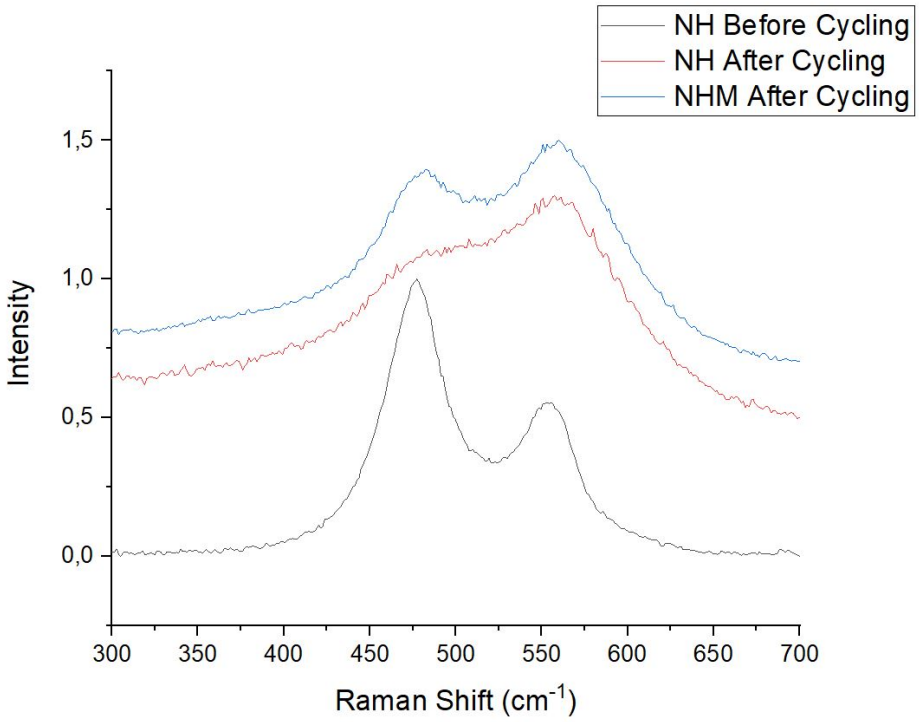

Figure 5.2. Comparison of raman spectra of NH electrode before and after 1000 cycles and NHM electrode after 1000 cycles.

In order to further elaborate the performance improvements of NHM electrode, electrochemical impedance spectroscopy results are compared (Figure 5.2). Among these graphs, NHM electrode before and after cycling shows the lowest R_s which can explain the improved specific capacitance (Table 5.1). R_s represents the internal resistance of the electrode, ionic resistance of the electrolyte and contact resistance within the electrode. Mxene flakes can promote a conductive network between nickel oxyhydroxide and more active sites to improve the contact between electrode and electrolyte, which would help to improve ion diffusion and electron transport during cycling [5]. Improved ion diffusion properties can be also observed by

checking the slope of the EIS data in the low frequency region. NHM before cycling obviously possesses the highest slope which means better diffusion properties.

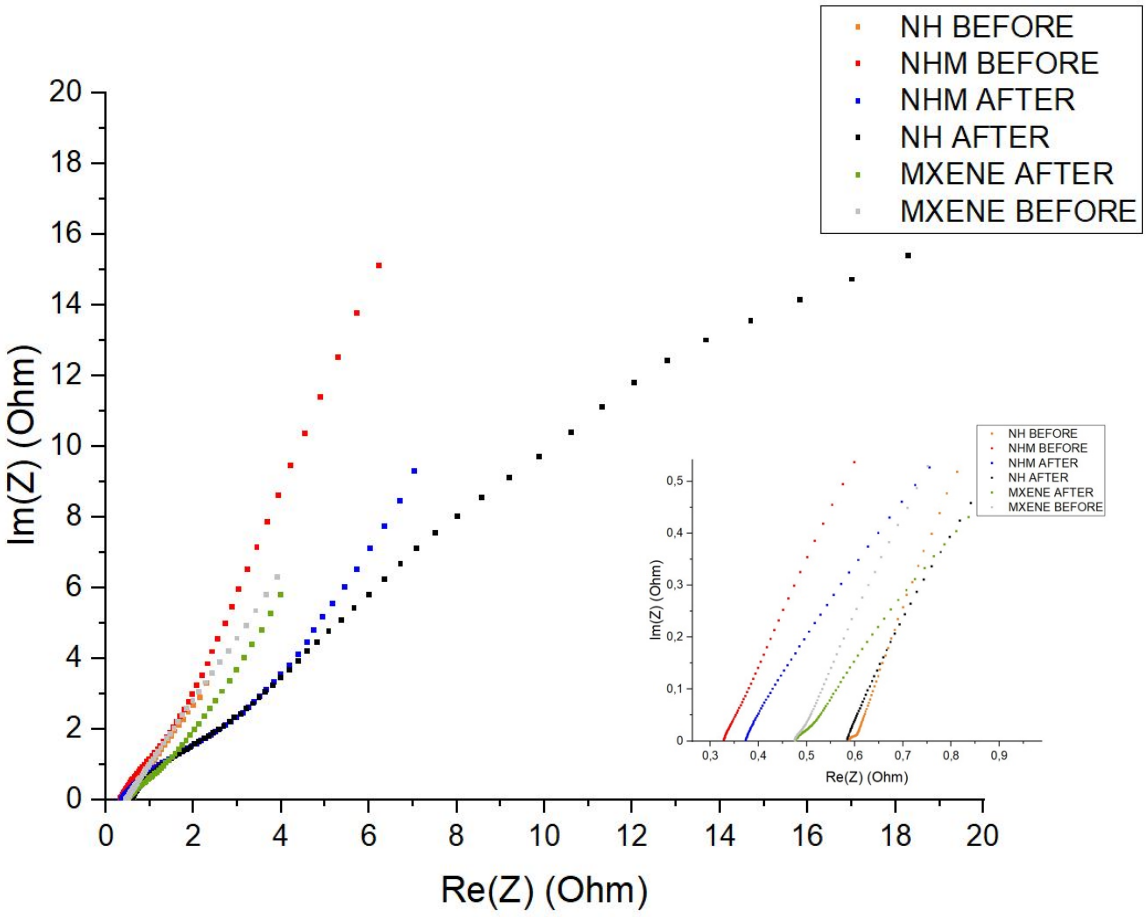

Figure 5.3. Nyquist plot of NH, NHM and mxene electrodes before and after 1000 cycles.

Table 5.1. Resistances of NH, mxene and NHM electrodes before and after 1000 cycles.

Sample	R_s before cycling	R_s after cycling	R_{ct} before cycling	R_{ct} after cycling
NH	0.642 Ω	0.584 Ω	0.015 Ω	2.397 Ω
Mxene	0.474 Ω	0.478 Ω	0.031 Ω	0.149 Ω
NHM	0.329 Ω	0.372 Ω	0.019 Ω	1.752 Ω

Scan rate dependent capacitances are calculated in order to obtain information about rate capabilites of the electrodes.(Table 5.2) . Rate capability is useful to gain information about power density of the electrodes [68]. According to results NH electrodes capacitance drops to 12% of the initial capacitance when scan rate is increased from 1 mv/s to 100 mv/s. Meanwhile, mxene electrode drops to 24% and NHM electrode drops to 16% of its capacitance that is calculated at 1 mv/s scan rate. This results shows the improved power density of the NHM electrode that can be a result of higher surface area which can faciliate the easier transport of electrons and ions.[68]

Table 5.2. Scan rate dependent areal capacitances of NH, mxene and NHM electrodes.

Sample	1 mv/s	5 mv/s	10 mv/s	20 mv/s	50 mv/s	100 mv/s
NH	4.61 F/cm^2	2.11 F/cm^2	1.59 F/cm^2	1.19 F/cm^2	0.92 F/cm^2	0.57 F/cm^2
Mxene	1.01 F/cm^2	0.60 F/cm^2	0.51 F/cm^2	0.41 F/cm^2	0.31 F/cm^2	0.24 F/cm^2
NHM	7.23 F/cm^2	3.55 F/cm^2	2.72 F/cm^2	2.02 F/cm^2	1.70 F/cm^2	1.21 F/cm^2

Overall, mxene coatings to the nickel oxyhydroxide electrodes improves the spesific capacitance however does not contribute to the capacity retention. Increased surface area of the electrode promotes the ion diffusion properties and also provides a connective network between nickel oxyhydroxide particles. Meanwhile, surface functional groups of the mxene flakes contributes to the faradaic reactions.

6. CONCLUSIONS AND RECOMMENDATIONS

- Electroactive materials are produced with binder free method in every production step in order to avoid using binders that would reduce the performance of the electrodes. Nickel oxyhydroxides are produced directly on the nickel foam surface by the anodic oxidation and mxenes are coated by using electrophoretic deposition.

- NH electrode provided a high capacitance of 1.15 F/cm^2 however, due to phase transformations that occur during cyling capacitance dropped to the 0.539 F/cm^2.

- Mxenes ($Ti_3C_2T_x$) are produced by LiF+HCl method and optimum production parameters are set at 12M LiF/ 9M HCl at 45ºC.

- Electrophoretic deposition method has been used and optimum parameters are set at electrolyte consists of 0.003 g I_2 in 50mL acetone by using 50V for 5 minutes. Increasing iodine causes bubble formation which greatly reduces the coating capabilities as well as damaging the flowerlike structure of nickel oxyhydroxide.

- Mxene electrode provided 0.41 F/cm^2 capacitance and it dropped to 0.298 F/cm^2 after 1000 cycling as a result of the oxidation of mxenes during cycling.

- By coating mxenes flakes on the nickel oxyhdroxide electrode an improvement in capacitance is achieved (1.91 F/cm^2 at 20 mv/s). The capacitance of the electrode can go up to 7.23 F/cm^2 when cycled at 1mV/s. Mxene flakes are coated on the flowerlike structure of nickel oxyhydroxide.

- All electrodes are cycled with different scan rates in order to obtain information about the reaction mechanism for energy storage. As a result, all three electrodes reaction mechanisms characterized as both diffusion and surface controlled. However, since slope of the logi vs log scan rate graphs are closer to 0.5, it is understood that diffusions' impact is higher.

- Improved surface area of the electrode is reflected on the solution resistance of the electrode which is 0.329 Ω before cyling and increases to 0.372 Ω after 1000 cycles. Meanwhile, diffusion properties of composite electrode is improved as the slope of the warburg line in the low frequency region is the highest in the case of NHM.
- Improvement of the diffusion properties are also reflected in rate capabilities since NH electrode can keep 12% of its capacitance when scan rate is increased from 1 mv/s to 100 mv/s while NHM electrode can keep 16% of its capacitance when scan rate is increased in the same manner.
- Overall, mxene coatings on NH improves the diffusion properties which greatly reflects to the performance of the NHM electrode. However, contributions has no effect on the capacity retention properties.

7. REFERENCES

[1] **H. Marin S. and J. C. Ellenbogen,** (2006) .“Supercapacitors : A Brief Overview,” .

[2] **Y. Wang, Y. Song, and Y. Xia,** (2016). “Electrochemical capacitors: mechanism, materials, systems, characterization and applications,” *Chem. Soc. Rev.*, vol. 45, pp. 5925–5950.

[3] **C. Soc, G. Wang, and J. Zhang,** (2012). “A review of electrode materials for electrochemical supercapacitors,” *Chem. Soc. Rev.*, pp. 797–828, 2012.

[4] **Q. X. Xia, J. Fu, M. Yun, S. Mane, and K. Ho,** (2017) .“High volumetric energy density annealed-MXene- nickel oxide/MXene asymmetric supercapacitor,” pp. 11000–11011.

[5] **Y. Wang *et al.*,** (2016). “Three-dimensional porous MXene/layered double hydroxide composite for high performance supercapacitors,” *J. Power Sources*, vol. 327, pp. 221–228.

[6] **X. Chen, R. Paul, and L. Dai,** (2017). “Carbon-based supercapacitors for efficient energy storage,” *Natl. Sci. Rev.*,

[7] **Samsudin, Nurul Asma. (2015).** Titania Nanotubes Synthesised via Electrochemical Anodisation Method: Synthesis and Supercapacitor Application. Pertanika Journal of Scholarly Research Reviews. 2. 107-128.

[8] **S. J. Moura, J. B. Siegel, D. J. Siegel, H. K. Fathy and A. G. Stefanopoulou,** (2010). "Education on vehicle electrification: Battery Systems, Fuel Cells, and Hydrogen," 2010 IEEE Vehicle Power and Propulsion Conference, Lille, 2010, pp. 1-6, doi: 10.1109/VPPC.2010.5729150.

[9] **C. Kunfeng and X. Dongfeng,** (2014) . “An Era of Powerful Supercapacitors : Materials Science and Engineering toward the System-Level Design of Ionic Supercapacitor Electrode and Electrolyte,” vol. 1, no. 1, pp. 3–5,

[10] **M. Forghani and S. W. Donne,** (2018) “Method Comparison for Deconvoluting Capacitive and Pseudo-Capacitive Contributions to Electrochemical Capacitor Electrode Behavior,” vol. 165, no. 3, pp. 664–673.

[11] **M. R. Lukatskaya, B. Dunn, and Y. Gogotsi,** (2016). “Multidimensional materials and device architectures for future hybrid energy storage,” *Nat. Commun.*, vol. 7.

[12] **V. Augustyn and B. Dunn,** (2014). "Pseudocapacitive oxide materials for high-rate electrochemical energy storage," *Energy Environ. Sci.*, pp. 1597–1614.

[13] **T. Brousse, D. Bélanger, and J. W. Long,** (2015). "To Be or Not To Be Pseudocapacitive?," *J. Electrochem. Soc.*, vol. 162, no. 5, pp. A5185–A5189.

[14] **N. M. Vinay Gupta,** (2013)"Polyaniline/single-wall carbon nanotube (PANI/SWCNT) composites for high performance supercapacitors,"

[15] **G. A. Snook, P. Kao, and A. S. Best,** (2011). "Conducting-polymer-based supercapacitor devices and electrodes," *J. Power Sources*, vol. 196, no. 1, pp. 1–12.

[16] **P. Sharma and T. S. Bhatti,** (2010) "A review on electrochemical double-layer capacitors," *Energy Convers. Manag.*, vol. 51, no. 12, pp. 2901–2912.

[17] **B.E.Conway,** (1999). "Electrochemical supercapacitors". New York: Kluwer Academic/ Plenum Press, 1999.

[18] **V. Gupta and N. Miura,** (2006) "Polyaniline / single-wall carbon nanotube (PANI / SWCNT) composites for high performance supercapacitors," vol. 52, pp. 1721–1726.

[19] **K. Rajendra and N. Miura,** (2004). "Polyaniline-MnO 2 Composite Electrode for High Energy Density Electrochemical Capacitor," pp. 425–428, 2004.

[20] **D. S. Hall, D. J. Lockwood, B. Christina, and B. R. MacDougall,** (2015). "Nickel hydroxides and related materials: a review of their structures, synthesis and properties," *Proc. R. Soc. A Math. Phys. Eng. Sci.*, vol. 471, no. 2174, p. 20140792.

[21] **H. Huang, Y. Guo, and Y. Cheng,** (2018). "Ultrastable α phase nickel hydroxide as energy storage materials for alkaline secondary batteries," *Appl. Surf. Sci.*, vol. 435, pp. 635–640.

[22] **S. W. Kim, I. H. Kim, S. I. Kim, and J. H. Jang,** (2017). "Nickel Hydroxide Supercapacitor with a Theoretical Capacitance and High Rate Capability Based on Hollow Dendritic 3D-Nickel Current Collectors," *Chem. - An Asian J.*, vol. 12, no. 12, pp. 1291–1296.

[23] **N. Tokmak and M. Urgen,** (2017). "Production and Characterization of Electroactive Nickel Oxides Grown on Nickel Foam by Anodic Oxidation in KOH Melts for Supercapacitor Applications," *MRS Adv.*, vol. 2, no. 54, pp. 3237–3247.

[24] **Sun, B., He, X., Leng, X., Jiang, Y., Zhao, Y., Suo, H., & Zhao, C.** (2016). Flower-like polyaniline–NiO structures: a high specific capacity supercapacitor electrode material with remarkable cycling stability. *RSC advances*, *6*(50), 43959-43963.

[25] **Pang, J., Mendes, R. G., Bachmatiuk, A., Zhao, L., Ta, H. Q., Gemming, T., ... & Rummeli, M. H.** (2019). Applications of 2D MXenes in energy conversion and storage systems. *Chemical Society Reviews*, *48*(1), 72-133.

[26] **D. Magne, P. Chartier, T. Cabioc'h, S. Célérier, and V. Mauchamp,** (2016) " Site-projected electronic structure of two-dimensional Ti 3 C 2 MXene: the role of the surface functionalization groups ," *Phys. Chem. Chem. Phys.*, vol. 18, no. 45, pp. 30946–30953.

[27] **Y. Dall, M. R. Lukatskaya, K. M. Cook, P. Taberna, Y. Gogotsi, and P. Simon,** (2014). "High capacitance of surface-modified 2D titanium carbide in acidic electrolyte," *Electrochem. commun.*, vol. 48, pp. 118–122.

[28] **H. Yu, Y. Wang, Y. Jing, J. Ma, C. Du, and Q. Yan,** (2019). "Surface Modified MXene-Based Nanocomposites for Electrochemical Energy Conversion and Storage," vol. 1901503, pp. 1–20.

[29] **L. Verger, C. Xu, V. Natu, H. Cheng, W. Ren, and M. W. Barsoum,** (2019). "Current Opinion in Solid State & Materials Science Overview of the synthesis of MXenes and other ultrathin 2D transition metal carbides and nitrides," *Curr. Opin. Solid State Mater. Sci.*, vol. 23, no. 3, pp. 149–163.

[30] **Xu, C., Wang, L., Liu, Z., Chen, L., Guo, J., Kang, N., ... & Ren, W.** (2015). Large-area high-quality 2D ultrathin Mo 2 C superconducting crystals. *Nature materials,* 14(11), 1135-1141.

[31] **L. Verger, M. W. Barsouma, H. Cheng, W. Ren, C. Xu, and V. Natu,** (2019). "Overview of the synthesis of MXenes and other ultrathin 2D transition metal carbides and nitrides," *Curr. Opin. Solid State Mater. Sci.*, vol. 23, no. 3, pp. 149–163.

[32] **Zhang, F., Zhang, Z., Wang, H., Chan, C. H., Chan, N. Y., Chen, X. X., & Dai, J. Y.** (2017). Plasma-enhanced pulsed-laser deposition of single-crystalline M o 2 C ultrathin superconducting films. Physical Review Materials, 1(3), 034002.

[33] **Alhabeb, M., Maleski, K., Anasori, B., Lelyukh, P., Clark, L., Sin, S., & Gogotsi, Y.** (2017). Guidelines for synthesis and processing of two-dimensional titanium carbide (Ti3C2T x MXene). Chemistry of Materials, 29(18), 7633-7644.

[34] **M. A. Hope, A. C. Forse, K. J. Griffith, M. R. Lukatskaya, M. Ghidiu, and C. P. Grey,** (2016). "NMR reveals the surface functionalisation of Ti 3 C 2," *Phys. Chem. Chem. Phys.*, vol. 18, pp. 5099–5102.

[35] **Xu, S., Wei, G., Li, J., Ji, Y., Klyui, N., Izotov, V., & Han, W. (**2017). Binder-free Ti3C2Tx MXene electrode film for supercapacitor produced by electrophoretic deposition method. *Chemical Engineering Journal*, 317, 1026-1036.

[36] **Naguib, M., Mashtalir, O., Lukatskaya, M. R., Dyatkin, B., Zhang, C., Presser, V., ... & Barsoum, M. W.** (2014). One-step synthesis of nanocrystalline transition metal oxides on thin sheets of disordered graphitic carbon by oxidation of MXenes. *Chemical communications*, 50(56), 7420-7423.

[37] **S. Huang and V. N. Mochalin,** (2019). "Hydrolysis of 2D Transition-Metal Carbides (MXenes) in Colloidal Solutions," *Inorg. Chem.*, vol. 58, pp. 1958–1966.

[38] **Habib, T., Zhao, X., Shah, S. A., Chen, Y., Sun, W., An, H., ... & Green, M. J.** (2019). Oxidation stability of Ti 3 C 2 T x MXene nanosheets in solvents and composite films. npj *2D Materials and Applications*, 3(1), 1-6.

[39] **M. Seredych, C. E. Shuck, D. Pinto, M. Alhabeb, and E. Precetti,** (2019). "High-Temperature Behavior and Surface Chemistry of Carbide MXenes Studied by Thermal Analysis," *Chem. Mater.*, vol. 31, pp. 3324–3332.

[40] **Lukatskaya, M. R., Kota, S., Lin, Z., Zhao, M. Q., Shpigel, N., Levi, M. D., ... & Gogotsi, Y.** (2017). Ultra-high-rate pseudocapacitive energy storage in two-dimensional transition metal carbides. *Nature Energy,* 2(8), 1-6.

[41] **Xie, Y., Naguib, M., Mochalin, V. N., Barsoum, M. W., Gogotsi, Y., Yu, X., ... & Kent, P. R.** (2014). Role of surface structure on Li-ion energy storage capacity of two-dimensional transition-metal carbides. J*ournal of the American Chemical Society,* 136(17), 6385-6394.

[42] **M. Naguib *et al.*,** (2013) . "New Two-Dimensional Niobium and Vanadium Carbides as Promising Materials for Li-Ion Batteries," pp. 8–11.

[43] **Q. Tang, Z. Zhou, and P. Shen,** (2012). "Are MXenes Promising Anode Materials for Li Ion Batteries ? Computational Studies on Electronic Properties and Li Storage Capability of Ti 3 C 2 and Ti 3 C 2 X 2 (X = F , OH) Monolayer," vol. 2.

[44] **Z. Lin, D. Sun, Q. Huang, J. Yang, M. Barsoum, and X. Yang,** (2012). "Carbon nanofibers bridged two-dimensional titanium carbide as a superior anode in lithium-ion battery," *J. Mater. Chem. A*,

[45] **F. Wang *et al.*,** (2017). "Facile synthesis SnO 2 nanoparticle-modified Ti 3 C 2 MXene nanocomposites for enhanced lithium storage application," *J. Mater. Sci.*, vol. 52, no. 7, pp. 3556–3565.

[46] **I. Type, H. Dalaver, and N. Energy,** (2017). "Atomic Layer Deposition of SnO2 on MXene for Li-Ion Battery Anodes," *Nano Energy*.

[47] **M. Okubo *et al.*,**(2016). "Sodium-Ion Intercalation Mechanism in MXene Nanosheets," *ACS Nano*, vol. 10, no. 3, pp. 3334–3341.

[48] **X. Xie *et al.*,** (2016). "Porous Heterostructured MXene/Carbon Nanotube Composite Paper with High Volumetric Capacity for Sodium-Based Energy Storage Devices," *Nano Energy*.

[49] **M. Naguib *et al.*,** (2017). "Electrochemical Performance of MXenes as K-ion Battery Anodes," *Chem. Commun.*, no. 51.

[50] **M. R. Lukatskaya *et al.*,** (2013) "Cation Intercalation and High Volumetric Capacitance of Two-Dimensional Titanium Carbide," vol. 341, pp. 1502–1504.

[51] **M. Ghidiu, M. R. Lukatskaya, M.-Q. Zhao, Y. Gogotsi, and M. W. Barsoum,** (2014) "Conductive two-dimensional titanium carbide 'clay' with high volumetric capacitance," *Nature*, vol. 516, pp. 76–81.

[52] **Okubo, M., Sugahara, A., Kajiyama, S., & Yamada, A.** (2018). MXene as a charge storage host. Accounts of chemical research, 51(3), 591-599.

[53] **M. R. Lukatskaya, S.-M. Bak, X. Yu, X.-Q. Yang, M. W. Barsoum, and Y. Gogotsi,** (2015). "Probing the Mechanism of High Capacitance in 2D Titanium Carbide Using In Situ X-Ray Absorption Spectroscopy," *Adv. Energy Mater.*

[54] **M. Hu, Z. Li, T. Hu, S. Zhu, C. Zhang, and X. Wang,** (2016). "High-Capacitance Mechanism for Ti3C2Tx MXene by in Situ Electrochemical Raman Spectroscopy Investigation," *ACS Nano*, vol. 10, no. 12, pp. 11344–11350.

[55] **B. Anasori, M. R. Lukatskaya, and Y. Gogotsi,** (2017). "2D metal carbides and nitrides (MXenes) for energy storage," *Nat. Rev. Mater.*, 2017.

[56] **R. B. Rakhi, B. Ahmed, M. N. Hedhili, D. H. Anjum, and H. N. Alshareef,** (2015) ."Effect of Postetch Annealing Gas Composition on the Structural and Electrochemical Properties of Ti 2 CT," *Chem. Mater.*

[57] **Q. X. Xia, J. Fu, J. M. Yun, R. S. Mane, and K. H. Kim,** (2017) "High Volumetric Energy Density Annealed-MXene-Nickel Oxide / MXene Asymmetric Supercapacitor," *RSC Adv.*, pp. 1–13.

[58] **Z. Ling, C. E. Ren, M. Zhao, J. Yang, J. M. Giammarco, and J. Qiu,** (2014) "Flexible and conductive MXene films and nanocomposites with high capacitance," pp. 1–6.

[59] **X. Zhao *et al.*,** (2015). "Fabrication of layered Ti3C2 with an accordion-like structure as a potential cathode material for high performance lithium–sulfur batteries," *J. Mater. Chem. A*, pp. 7870–7876.

[60] **T. Zhang, L. Pan, H. Tang, F. Du, Y. Guo, and T. Qiu,** (2017). "Synthesis of two-dimensional Ti 3 C 2 T x MXene using HCl & LiF etchant : Enhanced exfoliation and delamination," *J. Alloys Compd.*, vol. 695, pp. 818–826,.

[61] **E. G. Kalinina and E. Y. Pikalova**, (2019). "New trends in the development of electrophoretic deposition method in the solid oxide fuel cell technology: theoretical approaches, experimental solutions and development prospects," *Russ. Chem. Rev.*, vol. 88, no. 12, pp. 1179–1219.

[62] **M. W. Louie and A. T. Bell,** "An Investigation of Thin-Film Ni − Fe Oxide Catalysts for the Electrochemical Evolution of Oxygen," 2013.

[63] **Simon, P., Gogotsi, Y., & Dunn, B.** (2014). Where do batteries end and supercapacitors begin?. Science, 343(6176), 1210-1211

[64] **A. Viswanthan and A. N. Shetty,** (2018)**.** "Electrochemical comparison of nickel and nickel hydroxide nanoparticles composited with reduced graphene oxide and polyaniline for their supercapacitor application," *AIP Conf. Proc.*, vol. 1943, pp. 1–8,.

[65] **A. Motori, F. Sandrolini, and G. Davolio,** (1994). "Electrical properties of nickel hydroxide for alkaline cell systems," *J. Power Sources*, vol. 48, no. 3, pp. 361–370.

[66] **L. Lorencova *et al.*,** (2017) "Electrochemical performance of Ti3C2Tx MXene in aqueous media: towards ultrasensitive H2O2 sensing," *Electrochim. Acta*,.

[67] **P. Yan, R. Zhang, J. Jia, C. Wu, A. Zhou, and J. Xu,** (2015). "Enhanced supercapacitive performance of delaminated two-dimensional titanium carbide / carbon nanotube composites in alkaline electrolyte," *J. Power Sources*, vol. 284, pp. 38–43.

[68] **A. Yavuz, N. Ozdemir, P. Yilmaz, E. Huseyin, Z. Gulay, and Z. Metin,** (2019). "Nickel - based materials electrodeposited from a deep eutectic solvent on steel for energy storage devices," *Appl. Phys. A*, vol. 125, no. 8, pp. 1–10,.

CURRICULUM VITAE

Name Surname **:Berke KARAMAN**

Place and Date of Birth **: Istanbul, 31/03/1995**

E-Mail **: karaman.berke@gmail.com**

EDUCATION **:**

- **B.Sc.** **:** 2018, Istanbul Technical University, Metallurgical and Materials Engineering
- **M.Sc.** **:** 2020, Istanbul Technical University, Materials Engineering

PROFESSIONAL EXPERIENCE AND REWARDS:

- "The Scientific and Technological Research Council of Turkey" scholarship with joint project by Josef-Stefan Institute *"Innovative coatings for bare metallic vascular stents for reduction of restenosis and acceleration of natural endothelization"* Jan 2019 -July 2020
- B/S/H Group, Research and Development Intern, June 2016 - August 2016
- EnerjiSA, Quality Control Intern, June 2017
- ITU Surface Treatment Lab, Lab Intern, Feb 2018– Mar 2018

OTHER PUBLICATIONS, PRESENTATIONS AND PATENTS:

- B. Karaman, "Contribution of polyaniline coating to the stability and performance of nickel hydroxide based supercapacitor electrodes", International Symposium on Materials for Energy Storage and Conversion 2019, Akyaka/Muğla (Oral presentation)